Received: 21 March 2020 | Revised: 3 May 2020 | Accepted: 8 May 2020

DOI: 10.1002/aoc.5835

Applied Organometallic Chemistry WILEY

FULL PAPER

Synthesis of *cis*-1,2-diol-type chiral ligands and their dioxaborinane derivatives: Application for the asymmetric transfer hydrogenation of various ketones and biological evaluation

Ahmet Kilic[1] | **Tuğba Ersayan Balci**[1] | **Nevin Arslan**[2] | **Murat Aydemir**[3] | **Feyyaz Durap**[3] | **Veysi Okumuş**[4] | **Recep Tekin**[5]

[1]Art and Science Faculty, Chemistry Department, Harran University, Sanliurfa, 63190, Turkey

[2]Department of Field Crops, Faculty of Agriculture, Şırnak University, Şırnak, 73000, Turkey

[3]Department of Chemistry, Science Faculty, Dicle University, Diyarbakir, 21280, Turkey

[4]Department of Biology, Faculty of Science and Art, University of Siirt, Siirt, 56100, Turkey

[5]Department of Infectious Diseases and Clinical Microbiology, DicleUniversity Faculty of Medicine, Diyarbakir, 21280, Turkey

Correspondence
Ahmet Kilic, Harran University, Chemistry Department, TR-63190 Sanlıurfa, Turkey.
Email: kilica63@harran.edu.tr

Two *cis*-1,2-diol-type chiral ligands **(T_1** and **T_2)** and their tri-coordinated chiral dioxaborinane **($T_{(1-2)}B_{(1-2)}$)** and four-coordinated chiral dioxaborinane adducts with 4-*tert*-butyl pyridine sustained by N → B dative bonds **($T_{(1-2)}B_{(1-2)}$-N)** were synthesized and characterized by various spectroscopic techniques such as NMR (^{1}H, ^{13}C, and ^{11}B), FT-IR and UV–Vis spectroscopy, LC–MS/MS, and elemental analysis. It was suggested that both ferrocene and trifluoromethyl groups played key roles in the catalytic and biological studies because they could tune the solubility of the chiral dioxaborinane complexes and adjust the strength of intermolecular interactions. To assess the biological activities of newly synthesized chiral dioxaborinane compounds, DPPH (2,2-diphenyl-1-picrylhydrazyl) radical scavenging, reducing power, antibacterial, DNA binding, and DNA cleavage activities were tested. Then, all chiral dioxaborinane complexes were investigated as catalysts for the asymmetric transfer hydrogenation of various ketones under suitable conditions. The results indicated that the chiral dioxaborinane catalysts performed well with high yields.

KEYWORDS

asymmetric transfer hydrogenation, biological activitieschiral dioxaborinanes*Cis*-1,2-diol-type chiral ligands

1 | INTRODUCTION

Boron compounds and their different derivatives are nowadays widely applied in synthetic chemistry and also found its way into a wide range of industrial processes due to unique properties, different chemical structures, spectroscopic properties, pharmaceutical applications, and rich history in catalytic chemistry.[1–3] In particular, various group-functionalized dioxaborinane derivatives are an important category of boron compounds, which attract the tremendous interest in different applications in the past decade.[1–5] Recent examples are 1:1 Lewis type spontaneous formation of B → N bonds formed from boronic esters and different amines, of which the former is derived from arylboronic acids and *cis*-1,2-diol derivatives.[6,7] This stabilization was attributed to the relief of ring strain upon the geometry change of boron center from trigonal planar to tetrahedral due to a single vacant p orbital and absence of nonbonding electrons, which at the same time diminishes the reactivity of the

dioxaborinane ring towards hydrolysis.[6–8] Because of the aforementioned reasons, starting from relatively simple reagents, dioxaborinane complexes containing an N → B dative bond have successfully been developed including fluorescence,[9] electrochemical,[10] enzyme-based sensing,[11] pharmaceutical applications,[12,13] catalytic applications,[14–17] antioxidant and antimicrobial applications[18–24] *etc.*

Based on our expertise in designing boron-containing compounds as homogeneous catalysts for organic conversions and active compounds for pharmaceutical studies,[25–28] we have extended our research interests to the design of stable boron-containing compounds as catalysts for the transfer hydrogenation of various ketones, and active compounds for biological applications. When it comes to homogeneous, heterogeneous and/or organocatalytic systems, previous catalytic studies appear to focus mostly on transition metal catalysts. In the recently published catalytic studies, there are many studies in which main group metal catalysts are used together with transition metal catalysts. For this purpose, in recent years, significant advances for developing a wide range of effective catalytic systems and improvement studies toward enhancing the selectivity and practicability of the main group of catalysts, especially boron catalysts, have been accomplished.[14–17] Besides, main-group elements (p-block elements) offer great potential since they allow the activation of various chemical bonds and, consequently enable chemical transformations.[29,30] In addition, boron-containing compounds have been explored as inhibitors for different biological targets and some of them were approved by FDA as the drugs to treat a variety of diseases such as multiple myeloma, cancer, etc.[31,32]

Because of their biological potential as antibacterial, antioxidant and other agents, three-coordinated dioxaborinane and four-coordinated dioxaborinane complexes containing N → B dative bonds were found to exhibit significant biological activities.[33–37] Also, similar compounds exhibited good cytotoxic effects on skin cancer and cervical cancer cells.[38] Therefore, the synthesis and application of boron compounds containing imine and other functional groups to biological studies still attract considerable interest among the scientists since their medical effects have not been exactly explored. Two *cis*-1,2-diol-type chiral ligands and their tri- and four-coordinated chiral dioxaborinane adducts with 4-tert-butyl pyridine sustained by N → B dative bonds successfully were synthesized and characterized by various spectroscopic techniques such as NMR (^{1}H, ^{13}C, and ^{11}B), FT-IR and UV–Vis spectroscopy, LC–MS/MS, and elemental analysis. After the characterization of all compounds, the *cis*-1,2-diol-type chiral ligands and their chiral dioxaborinane complexes have been tested for DPPH (2,2-diphenyl-1-picrylhydrazyl) radical scavenging, reducing power, antibacterial, DNA binding, and DNA cleavage activities. Then, the chiral dioxaborinane complexes were investigated as catalysts for the transfer hydrogenation of various ketones under suitable conditions.

2 | EXPERIMENTAL

2.1 | General considerations

All chemical solvents, starting materials and other chemicals used for synthesis were commercially available and obtained from commercial suppliers were used without any additional purification and any additional chemical process. For the synthesis of chiral dioxaborinane derivatives, all reactions requiring a dry atmosphere were performed under argon (Ar) atmosphere in standard Dean-Stark techniques. ^{1}H (at 400 MHz) and ^{13}C (at 100 MHz) NMR-spectra were recorded using an Agilent Technologies 400 MHz spectrometer in $CHCl_3$ or DMSO-d_6 with TMS as internal standard. ^{11}B NMR spectra were acquired at 192.5 MHz in DMSO-d_6 and at 23 °C temperature. Chemical shifts are given in parts per million (ppm). Coupling constants (*J* values) are given in Hertz (Hz). The FT-IR spectra were recorded on a Perkin-Elmer Two UATR-FT spectrophotometer in the range of 4,000 to 400 cm^{-1} at 25 °C with equipped ATR accessory. Specific rotations were taken on a Perkin-Elmer 341 model polarimetry. UV–Vis measurements were acquired on a Perkin-Elmer model Lambda 25 spectrophotometer in the range of 200 to 1,100 nm using quartz cuvettes at room temperature and C_2H_5OH with $CHCl_3$ have been selected as solvents. The mass spectra (LC–MS) were obtained through using a Shimadzu LC–MS/MS spectrometer by ESI technique. Elemental analysis was carried out on a Fissions EA 1108 CHNS-O instrument. Thin layer chromatography (TLC) was conducted on glass plates coated with silica gel. Melting points of all complexes have been determined in open capillary tubes on an Electrothermal 9,100 melting point apparatus and are uncorrected. GC analyses were performed on a Shimadzu GC 2010 Plus Gas Chromatograph equipped with cyclodex B (Agilent) capillary column (30 m x 0.32 mm I.D. x 0.25 μm film thickness). Racemic samples of alcohols were obtained by reduction of the corresponding ketones with $NaBH_4$ and used as the authentic samples for *ee* determination. The GC parameters for asymmetric transfer hydrogenation of ketones were as follows; initial temperature, 50 °C; initial time 1.1 min; solvent delay, 4.48 min; temperature ramp 1.3 °C/min; final temperature, 150 °C; initial time

2.2 min; temperature ramp 2.15 °C/min; final temperature, 250 °C; initial time 3.3 min; final time, 44.33 min; injector port temperature, 200 °C; detector temperature, 200 °C, injection volume, 2.0 μL.

2.2 | Synthesis of chiral ligands (T_1 and T_2)

The chiral ligands (**T_1** and **T_2**) were synthesized as are given procedure: (1.0 g, 7.24 mmol) of 3,4-Dihydroxybenzaldehyde for chiral ligands **(T_1** and **T_2)** was dissolved in methyl alcohol (30 mL) at room temperature and put into a tri-necked-flask, equipped with a nitrogen (N_2) connection. The mixtures were warmed and then the (R)-(+)-α-ethyl benzylamine (1.10 mL, 7.24 mmol) for chiral ligand **(T_1)** and (R)-(+)-α-methyl benzylamine (0.92 mL, 7.24 mmol) for chiral ligand **(T_2)** was added to each reaction balloon in the presence of three drops formic acid as catalyst. The reaction mixture was heated to reflux temperature for 6 h with continuous stirring and then the mixture cooled slowly to room temperature. Solvent was removed in vacuo yielding a crude oil and the crude oil was washed three times with diethyl ether with n-hexane, successively, and crystallized in CH_2Cl_2/C_2H_5OH (1:3) by slow evaporation afforded pure **(T_1** and **T_2)** chiral ligands.

T_1: Yield: 1.89 g (86%), M.p. = 109 °C, Elemental Analysis (calculated for $C_{16}H_{17}NO_2$) (F.W: 255.3 g/mol) (%): C, 75.27; H, 6.71; N, 5.49. Found: C, 75.24; H, 6.67; N, 5.54. LC–MS/MS (Scan ES^+): m/z = 256.1 $[M + H]^+$. FT-IR (ATR, υ_{max}-cm^{-1}): 3448–2,381 υ(O-H···OH), 3,062 and 3,032 υ (Ar-CH), 2,968–2,877 υ (Aliph-CH), 1,660 υ(C=N), 1,567–1,454 υ(C=C), and 1,114 υ(C-O). ^{1}H-NMR (400 MHz; $CHCl_3$): δ (ppm) = 9.65 (s, 2H, O*H*), 8.13 (s, 1H, *H*C=N), 7.49–6.71 (m, 8H, Ar-C*H*), 4.08 (t, 1H, *J* = 6.4 Hz, N-C*H*), 1.84–1.61 (m, 2H, -CH-CH_2), and 0.76 (t, 3H, *J* = 5.4 Hz, -CH_2-CH_3). ^{13}C-NMR (100 MHz; $CHCl_3$): δ (ppm) = 161.00 (H*C*=N), 152.17, 145.44, 141.38, 139.88, 129.16, 129.08, 128.87, 128.66, 128.53, 128.30, 127.96, 127.91, 127.77, 127.47, 127.23, 126.60, 126.55, 126.17, and 115.39 (Ar-*C*H), 64.35 (N-*C*H), 29.03 (-CH-*C*H_2), and 10.63 (-CH_2-*C*H_3). UV–Vis (λ_{max}/(nm), * = shoulder peak): 230, 277, 318 and 408 (C_2H_5OH); 242, 268, 305, 359* and 413 ($CHCl_3$).

T_2: Yield: 1.45 g (83%), M.p. = 114 °C, Elemental Analysis (calculated for $C_{16}H_{17}NO_2$) (F.W: 241.1 g/mol) (%): C, 74.67; H, 6.27; N, 5.81. Found: C, 74.62; H, 6.24; N, 5.77. LC–MS/MS (Scan ES^+): m/z = 242.1 $[M + H]^+$. FT-IR (ATR, υ_{max}-cm^{-1}): 3443–2,375 υ(O-H···OH), 3,059 and 3,031 υ (Ar-CH), 2,979–2,872 υ (Aliph-CH), 1,661 υ(C=N), 1,569–1,448 υ(C=C), and 1,115 υ(C-O). ^{1}H-NMR (400 MHz; $CHCl_3$): δ (ppm) = 9.64 (s, 2H, O*H*), 8.17 (s, 1H, *H*C=N), 7.23–6.70 (m, 8H, Ar-C*H*), 4.41–4.27 (q, 1H, N-C*H*), and 1.43 (s, 3H, -CH-CH_3). ^{13}C-NMR (100 MHz; $CHCl_3$): δ (ppm) = 160.70 (H*C*=N), 152.32, 145.49, 144.51, 142.44, 140.91, 129.09, 128.69, 128.29, 127.49, 126.08, 125.85, 125.26, and 115.39 (Ar-*C*H), 57.03 (N-*C*H), and 22.49 (-CH-*C*H_3). UV–Vis (λ_{max}/(nm), * = shoulder peak): 224, 279, 319 and 409 (C_2H_5OH); 243, 269, 307, 357* and 412 ($CHCl_3$).

2.3 | Synthesis of tri-coordinated chiral dioxaborinane compounds ($T_{(1-2)}B_{[1-2]}$)

To a 100 ml round-bottom flask with a nitrogen (N_2) connection, chiral ligands (**T_1**) (0.32 g, 1.24 mmol) with (**T_2**) (0.30 g, 1.24 mmol) and corresponding ferrocene boronic acid (0.29 g, 1.24 mmol) for dioxaborinane compounds (**T_1B_1** and **T_2B_1**), and 3,5-Bis (trifluoromethyl)phenyl boronic acid (0.33 g, 1.24 mmol) for dioxaborinane compounds (**T_1B_2** and **T_2B_2**), respectively, in toluene (70 ml) were stirred under reflux conditions for 24 hr using a Dean-Stark condenser in order to remove the water by-product. Then, the mixtures were cooled slowly to room temperature and these mixtures were stirred at room temperature for 12 hr. Within this time a colored precipitate appeared and kept standing overnight. The solvent was removed under reduced pressure. The residue was washed three times with 5 ml of n-hexane and diethyl ether and crystallized in CH_2Cl_2/C_2H_5OH (1:3) by slow evaporation. TLC analysis showed a single well-defined peak for tri-coordinated chiral dioxaborinane compounds (**$T_{(1-2)}B_{(1-2)}$**).

T_1B_1: Yield: 0.42 g (74%), M.p. = 141 °C, Elemental Analysis (calculated for $C_{26}H_{24}BFeNO_2$) (F.W: 449.1 g/mol) (%): C, 69.53; H, 5.39; N, 3.12. Found: C, 69.49; H, 5.35; N, 3.08. LC–MS/MS (Scan ES^+): m/z = 450.1 $[M + H]^+$. FT-IR (ATR, υ_{max}-cm^{-1}): FT-IR (ATR, υ_{max}-cm^{-1}): 3205 υ (Fer C-H), 3,089 and 3,029 υ (Ar-CH), 2,974–2,880 υ (Aliph-CH), 1,649 υ(C=N), 1,539–1,456 υ(C=C), 1,382 υ (Fer C-C), 1,263 υ(B-O), 1,109 υ(C-O), 817 υ(B-C) and 477 υ (Fer Fe-C). ^{1}H-NMR (400 MHz; DMSO-d_6): δ (ppm) = 8.28 (s, 1H, *H*C=N), 7.58–6.74 (m, 8H, Ar-C*H*), 4.48 (s, 1H, N-C*H*), 4.30 (s, 2H, Fer-C*H*), 4.16 (s, 2H, Fer-C*H*), 4.04 (s, 5H, Fer-C*H*), 2.18–1.89 (m, 2H, -CH-CH_2), and 0.88 (t, 3H, *J* = 5.4 Hz, -CH_2-CH_3). ^{13}C-NMR (100 MHz; DMSO-d_6): δ (ppm) = 158.21 (H*C*=N), 152.34, 143.85, 138.05, 137.82, 129.39, 129.26, 128.70, 128.28, 128.14, 127.86, 127.59, 127.25, 126.91, 125.81, 108.47, and 105.73 (Ar-*C*H), 73.90, 71.59, 68.60, and 68.23 (Fer-*C*H), 56.69 (N-*C*H), 29.69 (-CH-*C*H_2), and 11.30 (-CH_2-*C*H_3). ^{11}B NMR (DMSO-d_6, 192.5 MHz, 23 °C, δ ppm): 31.43. UV–Vis (λ_{max}/(nm),

* = shoulder peak): 218, 237*, 322 and 362 (C_2H_5OH); 244, 269*, 305, and 329 ($CHCl_3$).

T_2B_1: Yield: 0.38 g (70%), M.p. = 100 °C, Elemental Analysis (calculated for $C_{25}H_{22}BFeNO_2$) (F.W: 435.1 g/mol) (%): C, 69.01; H, 5.10; N, 3.32. Found: C, 68.97; H, 5.07; N, 3.28. LC–MS/MS (Scan ES^+): m/z = 435.2 $[M]^+$. FT-IR (ATR, υ_{max}-cm^{-1}): 3208 υ (Fer C-H), 3,062 and 3,028 υ (Ar-CH), 2,982–2,877 υ (Aliph-CH), 1,646 υ(C=N), 1,559–1,489 υ(C=C), 1,380 υ (Fer C-C), 1,261 υ(B-O), 1,109 υ(C-O), 819 υ(B-C) and 480 υ (Fer Fe-C). ^{1}H-NMR (400 MHz; DMSO-d_6): δ (ppm) = 8.31 (s, 1H, HC=N), 7.45–6.53 (m, 8H, Ar-CH), 4.45 (s, 1H, N-CH), 4.29 (s, 2H, Fer-CH), 4.17 (s, 2H, Fer-CH), 4.07 (s, 5H, Fer-CH), and 1.05 (s, 3H, -CH-CH_3). ^{13}C-NMR (100 MHz; DMSO-d_6): δ (ppm) = 158.44 (HC=N), 152.27, 142.12, 139.61, 129.21, 129.11, 128.94, 128.74, 128.57, 128.34, 127.61, 127.15, 126.96, 126.49, 126.38, 108.39, and 105.67 (Ar-CH), 73.83, 71.50, 68.53, and 68.16 (Fer-CH), 56.47 (N-CH), and 20.05 (-CH-CH_3), ^{11}B NMR (DMSO-d_6, 192.5 MHz, 23 °C, δ ppm): 30.78. UV–Vis (λ_{max}/(nm), * = shoulder peak): 220, 258*, 323 and 410 (C_2H_5OH); 246, 329, and 417* ($CHCl_3$).

T_1B_2: Yield: 0.42 g (71%), M.p. = 105 °C, Elemental Analysis (calculated for $C_{24}H_{18}BF_6NO_2$) (F.W: 477.1 g/mol) (%): C, 60.41; H, 3.80; N, 2.94. Found: C, 60.39; H, 3.76; N, 2.90. LC–MS/MS (Scan ES^+): m/z = 478.2 $[M + H]^+$. FT-IR (ATR, υ_{max}-cm^{-1}): 3067 and 3,040 υ (Ar-CH), 2,974–2,882 υ (Aliph-CH), 1,643 υ(C=N), 1,569–1,457 υ(C=C), 1,264 υ(B-O), 1,120 υ(C-O) and 819 υ(B-C). ^{1}H-NMR (400 MHz; DMSO-d_6): δ (ppm) = 8.68 (s, 1H, HC=N), 8.37–7.14 (m, 11H, Ar-CH), 4.10 (t, 1H, J = 5.8 Hz, N-CH), 1.93–1.64 (m, 2H, -CH-CH_2), and 0.85 (t, 3H, J = 5.4 Hz, -CH_2-CH_3). ^{13}C-NMR (100 MHz; DMSO-d_6): δ (ppm) = 160.77 (HC=N), 154.33, 141.27, 139.70, 137.93, 134.75, 131.79, 129.98, 129.22, 128.66, 127.74, 127.40, 126.83, 123.91, 122.75, 120.03, 116.56, 115.96, 107.91, and 106.19 (Ar-CH), 125.45 (-CF_3), 57.35 (N-CH), 27.90 (-CH-CH_2), and 11.14 (-CH_2-CH_3). ^{11}B NMR (DMSO-d_6, 192.5 MHz, 23 °C, δ ppm): 32.43. UV–Vis (λ_{max}/(nm), * = shoulder peak): 221, 241*, 285, 334, 401, and 524* (C_2H_5OH); 244, 264, 331, 410, and 518* ($CHCl_3$).

T_2B_2: Yield: 0.42 g (73%), M.p. = 114 °C, Elemental Analysis (calculated for $C_{23}H_{16}BF_6NO_2$) (F.W: 463.1 g/mol) (%): C, 59.64; H, 3.48; N, 3.02. Found: C, 59.60; H, 3.44; N, 2.96. LC–MS/MS (Scan ES^+): m/z = 464.2 $[M + H]^+$. FT-IR (ATR, υ_{max}-cm^{-1}): 3070 and 3,029 υ (Ar-CH), 2,984–2,869 υ (Aliph-CH), 1,644 υ(C=N), 1,575–1,453 υ(C=C), 1,266 υ(B-O), 1,123 υ(C-O) and 820 υ(B-C). ^{1}H-NMR (400 MHz; DMSO-d_6): δ (ppm) = 8.69 (s, 1H, HC=N), 8.37–7.31 (m, 11H, Ar-CH), 4.76–4.69 (q, 1H, N-CH), and 0.80 (d, 3H, J = 6.4 Hz, -CH-CH_3). ^{13}C-NMR (100 MHz; DMSO-d_6): δ (ppm) = 160.78 (HC=N), 154.33, 141.26, 139.69, 137.92, 134.73, 132.11, 130.31, 129.98, 129.20, 128.65, 127.73, 127.39, 127.16, 126.84, 123.87, 122.74, 120.03, 119.47, 116.36, 115.96, 114.84, 109.33, 108.27, 105.69, and 105.29 (Ar-CH), 125.45 (-CF_3), 56.25 (N-CH), and 27.89 (-CH-CH_3). ^{11}B NMR (DMSO-d_6, 192.5 MHz, 23 °C, δ ppm): 29.85. UV–Vis (λ_{max}/(nm), * = shoulder peak): 221, 246*, 289, 332, 399, and 527* (C_2H_5OH); 245, 331, 406, and 523* ($CHCl_3$).

2.4 | Synthesis of four-coordinated chiral dioxaborinane compounds ($T_{(1–2)}B_{(1–2)}$-N)

To a 100 ml round-bottom flask, a CH_2Cl_2 solution (40 ml) of compound **(T_1B_1)** (0.30 g, 0.67 mmol), compound **(T_2B_1)** (0.29 g, 0.67 mmol), compound **(T_1B_2)** (0.32 g, 0.67 mmol) and compound **(T_2B_2)** (0.31 g, 0.67 mmol) was slowly added to a mixture of 4-*tert*-butyl pyridine (1.0 ml, 0.67 mmol) in CH_2Cl_2 (10 ml) at room temperature, respectively and the mixtures were stirred under room temperature for 24 hr. Follow by, the solvent was removed under vacuum evaporator and the obtained crystals was washed three times with 5 ml of n-hexane and crystallized in $CHCl_3$/C_2H_5OH (1:3) by slow evaporation. TLC analysis showed a single well-defined peak for four-coordinated chiral dioxaborinane compounds **($T_{(1–2)}B_{(1–2)}$-N)**. The different spectral results allows assignment to the known 4-*tert*-butyl pyridine adduct of tri-coordinated chiral dioxaborinane compounds and tri-coordinated chiral dioxaborinane compounds **($T_{(1–2)}B_{(1–2)}$)** then converted into the corresponding four-coordinated chiral dioxaborinane compounds **($T_{(1–2)}B_{(1–2)}$-N)**.

T_1B_1-N: Yield: 0.32 g (82%), M.p. = 230 °C, Elemental Analysis (calculated for $C_{35}H_{37}BFeN_2O_2$) (F.W: 584.3 g/mol) (%): C, 71.94; H, 6.38; N, 4.79. Found: C, 71.91; H, 6.34; N, 4.72. LC–MS/MS (Scan ES^+): m/z = 584.3 $[M + H]^+$. FT-IR (ATR, υ_{max}-cm^{-1}): FT-IR (ATR, υ_{max}-cm^{-1}): 3221 υ (Fer C-H), 3,062 and 3,031 υ (Ar-CH), 2,968–2,871 υ (Aliph-CH), 1,643 υ(C=N), 1,566–1,451 υ(C=C), 1,365 υ (Fer C-C), 1,274 υ(B-O), 1,104 υ(C-O), 819 υ(B-C) and 483 υ (Fer Fe-C). ^{1}H-NMR (400 MHz; DMSO-d_6): δ (ppm) = 8.17 (s, 1H, HC=N), 7.68–6.96 (m, 12H, Ar-CH), 4.41 (s, 1H, N-CH), 4.28 (s, 2H, Fer-CH), 4.13 (s, 2H, Fer-CH), 4.04 (s, 5H, Fer-CH), 1.81–1.59 (m, 2H, -CH-CH_2), 1.24 (s, 9H, *t*-BuPy-CH_3), and 1.02 (s, 3H, -CH_2-CH_3). ^{13}C-NMR (100 MHz; DMSO-d_6): δ (ppm) = 159.79 (HC=N), 149.21, 138.09, 134.77, 132.98, 131.71, 129.11, 129.08, 128.99, 128.87, 128.67, 128.29, 127.80, 127.48, 127.13, 126.84, 125.42, 123.97, 122.76, 120.99, 111.45, and 106.20 (Ar-CH), 73.83, 71.49, 68.52, 68.33, (Fer-CH), 56.12 (N-CH), 34.48 (*t*-BuPy-C-

CH_3), 30.65 (*t*-BuPy-C-$\underline{C}H_3$), 29.46 (-CH-$\underline{C}H_2$), and 11.29 (-CH_2-$\underline{C}H_3$). ^{11}B NMR (DMSO-d_6, 192.5 MHz, 23 °C, δ ppm): 14.78. UV–Vis (λ_{max}/(nm), * = shoulder peak): 221, 254*, and 334 (C_2H_5OH); 248 and 346 ($CHCl_3$).

T_2B_1-N: Yield: 0.32 g (84%), M.p. = 298 °C, Elemental Analysis (calculated for $C_{25}H_{22}BFeN_2O_2$) (F.W: 570.3 g/mol) (%): C, 71.60; H, 6.19; N, 4.91. Found: C, 71.56; H, 6.15; N, 4.87. LC–MS/MS (Scan ES$^+$): m/z = 570.4 $[M]^+$. FT-IR (ATR, υ_{max}-cm^{-1}): 3216 υ (Fer C-H), 3,058 and 3,031 υ (Ar-CH), 2,971–2,869 υ (Aliph-CH), 1,646 υ(C=N), 1,548–1,451 υ(C=C), 1,378 υ (Fer C-C), 1,263 υ(B-O), 1,104 υ(C-O), 817 υ(B-C) and 486 υ (Fer Fe-C). ^{1}H-NMR (400 MHz; DMSO-d_6): δ (ppm) = 8.47 (s, 1H, $\underline{H}$C=N), 7.60–6.71 (m, 12H, Ar-C$\underline{H}$), 4.41 (s, 1H, N-C$\underline{H}$), 4.26 (s, 2H, Fer-C$\underline{H}$), 4.13 (s, 2H, Fer-C$\underline{H}$), 4.04 (s, 5H, Fer-C$\underline{H}$), and 1.24 (s, 9H, *t*-BuPy-C$\underline{H}_3$), 1.03 (s, 3H, -CH-C$\underline{H}_3$). ^{13}C-NMR (100 MHz; DMSO-d_6): δ (ppm) = 159.58 (H$\underline{C}$=N), 158.47, 152.29, 152.10, 142.19, 140.22, 139.75, 129.22, 129.02, 128.75, 128.30, 126.94, 126.41, 125.97, 108.40, and 105.68 (Ar-$\underline{C}$H), 73.85, 71.52, 68.55, and 68.18 (Fer-$\underline{C}$H), 53.87 (N-$\underline{C}$H), 34.90 (*t*-BuPy-$\underline{C}$-CH_3), 30.65 (*t*-BuPy-C-$\underline{C}H_3$), and 22.21 (-CH-$\underline{C}H_3$). ^{11}B NMR (DMSO-d_6, 192.5 MHz, 23 °C, δ ppm): 14.97. UV–Vis (λ_{max}/(nm), * = shoulder peak): 234, 256, 283*, and 321 (C_2H_5OH); 245, 325, and 358* ($CHCl_3$).

T_1B_2-N: Yield: 0.35 g (86%), M.p. = 140 °C, Elemental Analysis (calculated for $C_{24}H_{18}BF_6N_2O_2$) (F.W: 612.4 g/mol) (%): C, 64.72; H, 5.10; N, 4.57. Found: C, 64.69; H, 5.06; N, 4.51. LC–MS/MS (Scan ES$^+$): m/z = 613.4 $[M + H]^+$. FT-IR (ATR, υ_{max}-cm^{-1}): 3064 and 3,032 υ (Ar-CH), 2,973–2,878 υ (Aliph-CH), 1,638 υ(C=N), 1,575–1,458 υ(C=C), 1,265 υ(B-O), 1,118 υ(C-O) and 818 υ(B-C). ^{1}H-NMR (400 MHz; DMSO-d_6): δ (ppm) = 8.69 (s, 1H, $\underline{H}$C=N), 8.48–7.27 (m, 15H, Ar-C$\underline{H}$), 4.16 (t, 1H, *J* = 5.4 Hz, N-C$\underline{H}$), 2.04–1.68 (m, 2H, -CH-C$\underline{H}_2$), 1.22 (s, 9H, *t*-BuPy-C$\underline{H}_3$), and 0.79 (t, 3H, *J* = 5.4 Hz, -CH_2-C$\underline{H}_3$). ^{13}C-NMR (100 MHz; DMSO-d_6): δ (ppm) = 160.77 (H$\underline{C}$=N), 149.29, 138.03, 134.74, 132.08, 131.76, 129.98, 129.66, 129.31, 129.16, 129.04, 128.99, 128.95, 128.82, 128.66, 128.29, 127.80, 127.43, 127.17, 126.98, 126.84, 126.71, 123.91, 122.75, 121.39, 116.35 and 109.30 (Ar-$\underline{C}$H), 125.45 (-$\underline{C}F_3$), 56.25 (N-$\underline{C}$H), 34.93 (*t*-BuPy-$\underline{C}$-CH_3), 30.54 (*t*-BuPy-C-$\underline{C}H_3$), 27.90 (-CH-$\underline{C}H_2$), and 11.16 (-CH_2-$\underline{C}H_3$). ^{11}B NMR (DMSO-d_6, 192.5 MHz, 23 °C, δ ppm): 14.52. UV–Vis (λ_{max}/(nm), * = shoulder peak): 223, 251*, 330, 397 and 523* (C_2H_5OH); 242, 327, 404 and 513* ($CHCl_3$).

T_2B_2-N: Yield: 0.33 g (83%), M.p. = 120 °C, Elemental Analysis (calculated for $C_{32}H_{29}BF_6N_2O_2$) (F.W: 598.4 g/mol) (%): C, 64.23; H, 4.89; N, 4.68. Found: C, 64.19; H, 4.84; N, 4.61. LC–MS/MS (Scan ES$^+$): m/z = 599.4 $[M + H]^+$. FT-IR (ATR, υ_{max}-cm^{-1}): 3064 and 3,032 υ (Ar-CH), 2,974–2,871 υ (Aliph-CH), 1,636 υ(C=N), 1,574–1,454 υ(C=C), 1,262 υ(B-O), 1,121 υ(C-O) and 817 υ(B-C). ^{1}H-NMR (400 MHz; DMSO-d_6): δ (ppm) = 8.65 (s, 1H, $\underline{H}$C=N), 8.77–7.21 (m, 15H, Ar-C$\underline{H}$), 5.11–4.77 (q, 1H, N-C$\underline{H}$), 1.24 (s, 9H, *t*-BuPy-C$\underline{H}_3$), and 0.81 (s, 3H, -CH-C$\underline{H}_3$). ^{13}C-NMR (100 MHz; DMSO-d_6): δ (ppm) = 160.48 (H$\underline{C}$=N), 153.48, 149.21, 142.07, 140.85, 139.55, 134.76, 131.74, 129.32, 129.11, 128.95, 128.73, 128.68, 128.28, 128.04, 127.18, 127.12, 127.04, 126.63, 126.46, 126.34, 123.96, 122.75, 121.47, 116.37, and 115.95 (Ar-$\underline{C}$H), 125.46 (-$\underline{C}F_3$), 57.01 (N-$\underline{C}$H), 34.97 (*t*-BuPy-$\underline{C}$-CH_3), 30.52 (*t*-BuPy-C-$\underline{C}H_3$), and 21.10 (-CH-$\underline{C}H_3$). ^{11}B NMR (DMSO-d_6, 192.5 MHz, 23 °C, δ ppm): 14.55. UV–Vis (λ_{max}/(nm), * = shoulder peak): 219, 284, 330, 402, and 524* (C_2H_5OH); 241, 326, 408, and 521* ($CHCl_3$).

2.5 | Catalytic transfer hydrogenation

General procedure for the catalytic hydrogen-transfer reaction is given below: A solution of tri or four coordinated chiral dioxaborinane complexes (0.005 mmol), NaOH (0.025 mmol) and the corresponding ketone (0.5 mmol) in degassed *iso*-PrOH (5.0 ml) was refluxed until the reaction completed. Then, a sample of the reaction mixture is taken off, diluted with acetone, and analyzed immediately by GC; conversions obtained are related to the residual unreacted ketone.

2.6 | Biological assays

2.6.1 | DPPH radical scavenging activity

The stock solutions of the chiral dioxaborinane complexes were diluted in DMSO to a final concentration of 25–200 μg/ml. Methanol solution of 2.0 ml DPPH was added to 0.5 ml test complexes in different concentrations of dimethyl sulfoxide (DMSO) and incubated at room temperature for 40 min in the dark. After the incubation time, the absorbance of the solution was measured at 517 nm. Trolox was used as a reference standard substance to evaluate complexes.[39]

2.6.2 | Reducing power activity

The reducing power activity of the chiral dioxaborinane complexes was tested by the method of Oyaizu[40] with minor modifications. The stock solutions of the chiral dioxaborinane complexes were diluted to the working range concentrations (25–200 μg/ml) in DMSO and activity was determined at 700 nm. α-tocopherol was used as a standard.

2.6.3 | Antibacterial activity

Antibacterial activity of the chiral dioxaborinane complexes was tested according to Khan and Asiri.[41] Stock solutions of the compounds were prepared in DMSO at a concentration of 500 μg/ml. 15 μL of compounds impregnated into sterile antibiotic discs and each disc was placed in a petri dish with nutrient agar inoculated with bacteria. *Pseudomonas aeruginosa* (ATCC 9027), *Escherichia coli* (ATCC 10536) and *Legionella pneumophila* subsp. *pneumophiia* (ATCC 33152) were used as Gram-negative bacteria and *Enterococcus hirae* (ATCC 10541), *Staphylococcus aureus* (ATCC 6538) and *Bacillus cereus* were used as test microorganisms. Streptomycin (10 μg) and Tetracycline (30 μg) were used as reference standard antibiotics.

2.6.4 | DNA binding and DNA cleavage activities

DNA binding and DNA cleavage activities of the chiral dioxaborinane complexes were performed using agarose gel electrophoresis according to the method of Meriç et al.[42] The complexes prepared at 200 μg/ml in DMSO were incubated for 8 hr at 37 °C with CT-DNA at 2 μg/ml concentrations and pBR322 DNA at 0.1 μg/ml concentrations. Then, the samples were loaded on 1% agarose gel containing 8 μl 0.05% ethidium bromide, followed by displaying under UV light and photographing.

3 | RESULTS AND DISCUSSION

3.1 | Synthesis and characterization

Initially, two novel chiral ligands **(T_1** and **T_2)** were obtained from 3,4-dihydroxybenzaldehyde and (R)-(+)-α-ethyl benzylamine or (R)-(+)-α-methyl benzylamine in methyl alcohol under reflux temperature with a yield in the range 86–83% in the presence of three drops of formic acid as catalyst, as shown in Scheme 1. After crystallization and full characterization of the chiral ligands **(T_1** and **T_2)**, they were employed in the synthesis of the respective novel tri-coordinated chiral dioxaborinane complexes **($T_{(1-2)}B_{(1-2)}$)** in toluene under reflux conditions for 24 hr with a yield up to 74% (see Scheme 2) using a Dean-Stark condenser to remove the water by-product. Subsequently, as shown in Scheme 3, the four-coordinated chiral dioxaborinane compounds **($T_{(1-2)}B_{(1-2)}$-N)**, in which the boron is four-coordinated due to chelation by 4-*tert*-butyl pyridine group, were synthesized in CH_2Cl_2 at room temperature over 24 hr with a good yield in the range 86–82%. The novel tri-coordinated chiral dioxaborinane **($T_{(1-2)}B_{(1-2)}$)** and four-coordinated chiral dioxaborinane complexes **($T_{(1-2)}B_{(1-2)}$-N)**, in which boron is four-coordinated due to chelation by 4-*tert*-butyl pyridine group, were designed for spectroscopic and catalytic study as well as antimicrobial activities and antioxidant studies. The formed four-coordination bonds with 4-*tert*-butyl pyridine nucleophiles as well as covalent B-O and B-N bonds make the structure stable in air. The formation of the two *cis*-1,-2-diol-type chiral ligands **(T_1** and **T_2)** and their tri-coordinated chiral dioxaborinane compounds **($T_{(1-2)}B_{(1-2)}$)** and four-coordinated chiral dioxaborinane compounds **($T_{(1-2)}B_{(1-2)}$-N)**, in which boron is four-coordinated due to chelation by 4-*tert*-butyl pyridine group, were fully characterized using several spectroscopic and analytical techniques such as NMR (^{1}H, ^{13}C, and ^{11}B), FT-IR, and UV–Vis spectroscopy, LC–MS/MS, and elemental analysis. Attempts to grow crystals of the *cis*-1,2-diol-type chiral ligands **(T_1** and **T_2)** and their tri-coordinated chiral dioxaborinane **($T_{(1-2)}B_{(1-2)}$)** and

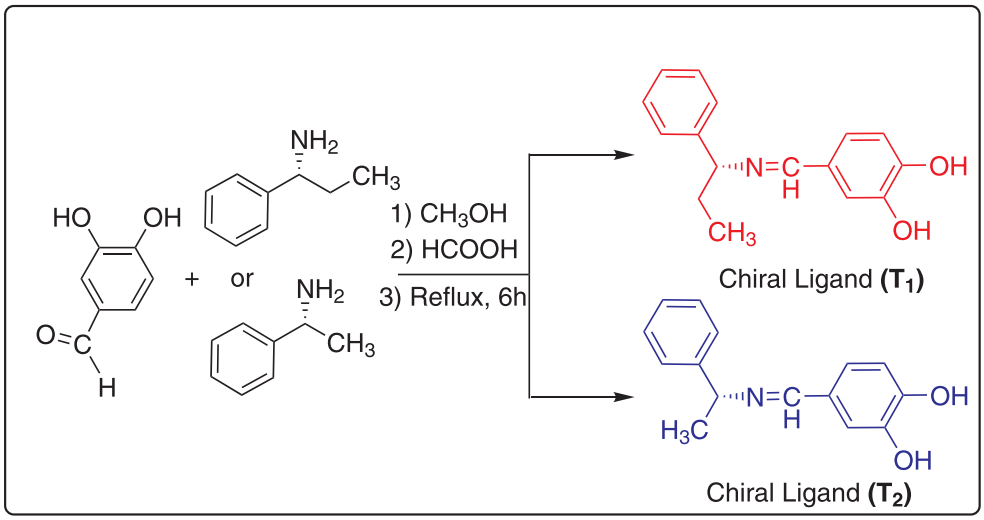

SCHEME 1 Synthesis route of proposed chiral ligands **(T_1** and **T_2)**

SCHEME 2 Synthesis of proposed tri-coordinated chiral dioxaborinane compounds **($T_{(1-2)}B_{(1-2)}$)**

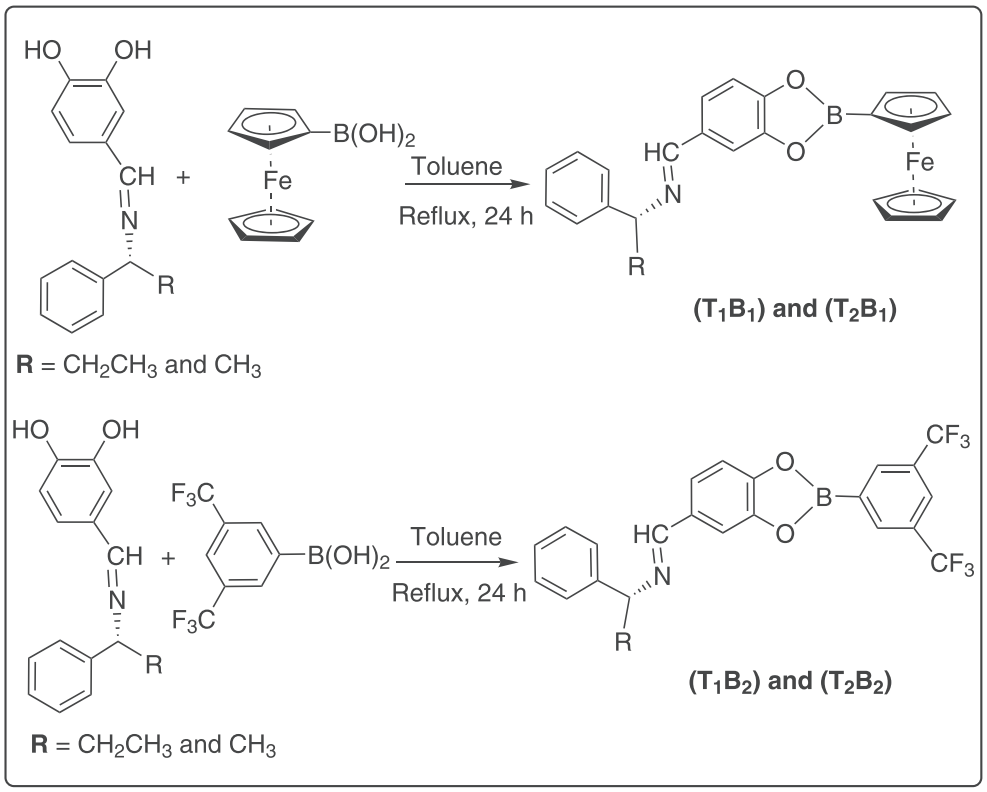

SCHEME 3 Structure of proposed four-coordinated chiral dioxaborinane compounds **($T_{(1-2)}B_{(1-2)}$-N)**

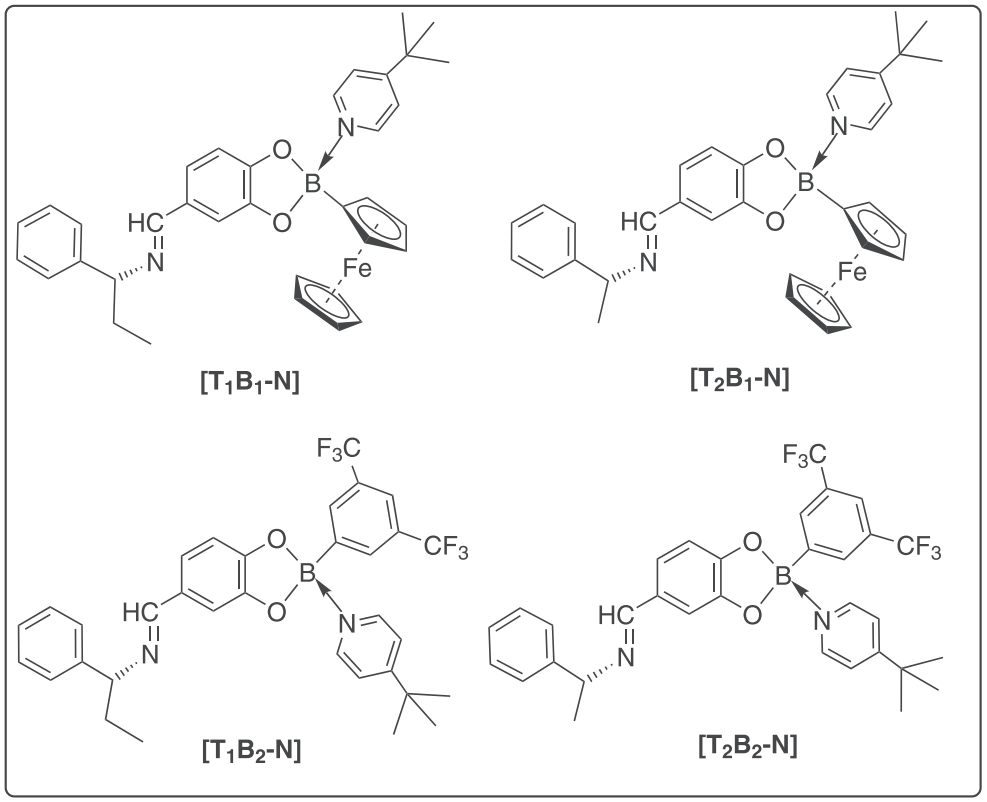

four-coordinated chiral dioxaborinane complexes **($T_{(1-2)}B_{(1-2)}$-N)** suitable for single-crystal XRD were not successful. However, the spectroscopic and analytical results of all compounds are consistent with the proposed structure. Also, all compounds were isolated as a powder that is air-stable in the solid-state and all compounds

were followed by TLC, which revealed that the compounds were sufficiently pure. Also, CHN elemental analysis supported purity of the compounds.

3.2 | Spectroscopic studies

FT-IR spectroscopy was used as a characteristic technique to elucidate structures of *cis*-1,2-diol-type chiral ligands **(T_1** and **T_2)** and their chiral dioxaborinane derivatives **($T_{(1-2)}B_{(1-2)}$)** and **($T_{(1-2)}B_{(1-2)}$-N)**, FT-IR spectral data of which are given in the experimental part. In the FT-IR spectra of **($T_{(1-2)}B_{(1-2)}$)** and **($T_{(1-2)}B_{(1-2)}$-N)**, a broad band of the ligands in the range of 3,448–2,334 cm^{-1}, which corresponded to the *cis*-1,2-diol υ(O-H⋯OH), completely disappeared. Other characteristic bands appeared at approximately 1,660 cm^{-1} correspond to the stretching vibrations of imine υ(C=N) group of chiral ligands **(T_1** and **T_2)**, whereas the imine υ(C=N) stretching vibrations of complexes **($T_{(1-2)}B_{(1-2)}$)** and **($T_{(1-2)}B_{(1-2)}$-N)** appeared in the range of 1,649–1,643 and 1,646–1,636 cm^{-1}, respectively.[16,43–45] Moreover, the two new characteristic peaks in the range of 1,274–1,261 and 820–817 cm^{-1} correspond to the stretching vibrations of υ(B-O) and υ(B-C) groups of chiral dioxaborinane derivatives **($T_{(1-2)}B_{(1-2)}$)** and **($T_{(1-2)}B_{(1-2)}$-N)**, respectively.[26,46] Furthermore, two peaks observed in the range of 1,382–1,365 and 486–480 cm^{-1}, which could be attributed to ferrocene υ(C-C) and υ (Fe-C) stretchings in the framework of chiral dioxaborinane complexes, respectively.Electronic transitions of ligands **(T_1** and **T_2)** and their chiral dioxaborinane **($T_{(1-2)}B_{(1-2)}$)** and **($T_{(1-2)}B_{(1-2)}$-N)** complexes were studied in C_2H_5OH and $CHCl_3$ (2.10^{-6}–2.10^{-8} M) at room temperature and recorded at λ_{max} as nm. The UV–Vis spectral data of all chiral compounds are given in Figure S17–22 and the experimental section. The chiral ligands and their boron complexes typically display a λ_{max} value of between 218 and 527 nm in their UV–Vis absorption spectra due to π → π*, n → π* transition of non-bonded electrons or π-to-vacant B p-orbital transitions. Besides, some specific transitions of π → π* and n → π* were observed in the range of 224–413 nm in C_2H_5OH or $CHCl_3$, respectively, for ligands **(T_1** and **T_2)** with little shift after bonding to the boron center. Additionally, in the electronic spectra of chiral dioxaborinane **($T_{(1-2)}B_{(1-2)}$)** and **($T_{(1-2)}B_{(1-2)}$-N)** complexes, the strong broad absorption bands in the range 218–527 nm in C_2H_5OH or $CHCl_3$ can be attributed to the π → π*, n → π* transition of non-bonded electrons or π-to-vacant B p-orbital transitions.[47] In view of the this results, the strong broad absorption bands in the range 218–346 nm in C_2H_5OH or $CHCl_3$, respectively, can be attributed to the π → π* transitions of aromatic benzene ring. The following the n → π* transition of non-bonded electrons of imine (C=N) groups or π-to-vacant B p-orbital transition was observed in the range 357–527 nm in C_2H_5OH or $CHCl_3$, respectively.[47]

The NMR (^1H, ^{13}C, and ^{11}B) spectral data were in good agreement with the proposed structures in $CDCl_3$ or DMSO-d_6 (Figure S1-S16 in the ESI). The major difference between the ^1H NMR spectra of ligands **(T_1** and **T_2)** and their complexes **($T_{(1-2)}B_{(1-2)}$)** and **($T_{(1-2)}B_{(1-2)}$-N)** is the presence of a new signal for the boronic acid groups and 4-*tert*-butyl pyridine (Figure S1-S10 in the ESI). In ^1H NMR spectra, the disappearance of a singlet at 9.65 and 9.64 ppm for **(T_1)** and **(T_2)**, respectively, which belong to -O*H* group of the *cis*-1,2-diol, is the indication for the deprotonation of hydroxyl and formation of the desired chiral dioxaborinane complexes, as expected.[15,48,49] The characteristic resonance of the azomethine (C*H*=N) protons shifted from 8.13 and 8.17 ppm for **(T_1)** and **(T_2)**, respectively, to 8.69–8.17 ppm in the chiral dioxaborinane complexes, indicating the formation of the complexes, as observed elsewhere.[50] Furthermore, the ferrocene region can show three signals in the range of 4.30–4.04 ppm due to the non-substituted cyclopentadiene of ferrocene-based chiral dioxaborinane **($T_{(1-2)}B_1$)** and **($T_{(1-2)}B_1$-N)** derivatives.[51] Moreover, the ^{13}C NMR spectra can be analyzed analogously to that of the proton spectra and the resonances in the ^{13}C NMR spectra support the formation of the ligands and their chiral dioxaborinane complexes (Figure S1-S10 in the ESI). In the ^{13}C NMR spectra, the signal of the imine carbon (*C*H=N) shifted after coordination to boron center from 161.00–160.70 ppm in ligands **(T_1** and **T_2)** to 160.78–158.21 ppm in complexes **($T_{(1-2)}B_{(1-2)}$)** and 160.77–159.58 in **($T_{(1-2)}B_{(1-2)}$-N)**. These results clearly show that the free ligands bound to the boron center in the chiral dioxaborinane complexes and the noticeable shift is observed for the (*C*H=N) resonance due to complexation, as expected. Specifically, in the ^{13}C NMR spectra of the ferrocene-based chiral dioxaborinane complexes **($T_{(1-2)}B_1$)** and **($T_{(1-2)}B_1$-N)**, the carbon signals of ferrocene unit were observed at range 73.90–68.16 ppm, confirming that two cyclopentadiene ring containing the ferrocene unit bound to boron center.[15] The other characteristic carbon resonances for the compounds were observed in the expected values, which is another evidence of the formation of the proposed structures. The ^{11}B NMR data also supports the formation of the chiral dioxaborinane complexes (Figures 1, 2 and S11–16 in the ESI). The ^{11}B NMR spectra are of special interest because the signal in the ^{11}B NMR spectra gives a strong indication of whether the complexes formed or not. As expected, the ^{11}B NMR spectra of tri-coordinated chiral dioxaborinanes **($T_{(1-2)}B_{(1-2)}$)** in DMSO-d_6

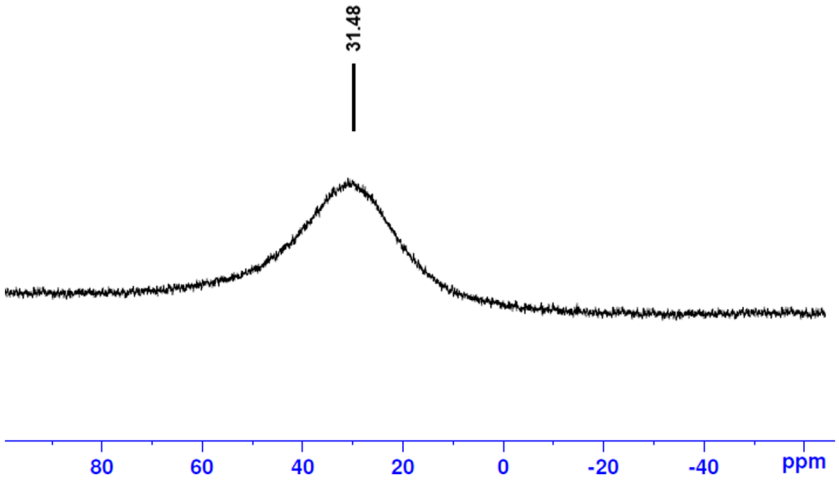

FIGURE 1 ^{11}B NMR spectrum of chiral dioxaborinane **(T_1B_1)**

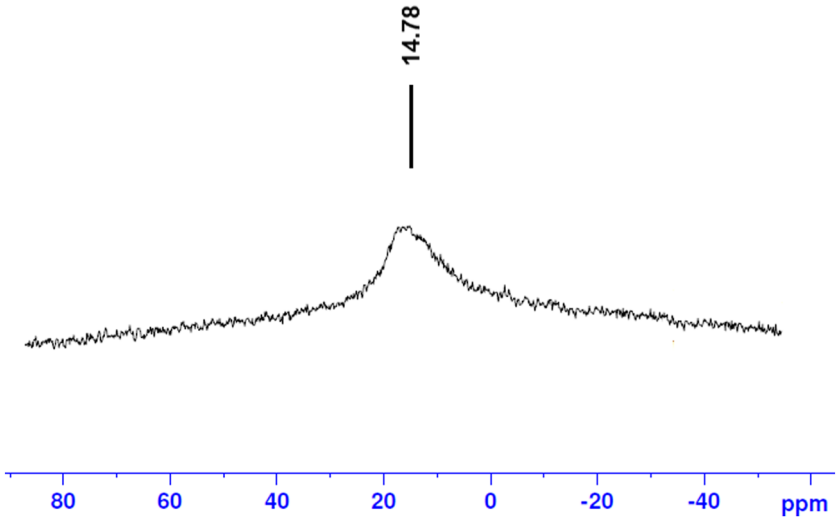

FIGURE 2 ^{11}B NMR spectrum of chiral dioxaborinane **(T_1B_1-N)**

exhibited only broad singlet signals in the range of 32.43–29.85 ppm for the trigonal geometry due to the similar chemical environment for the boron center of each chiral dioxaborinane complexes. On the other hand, the ^{11}B NMR spectra of four-coordinated chiral dioxaborinanes **($T_{(1-2)}B_{(1-2)}$-N)** showed only broad singlet resonances in the range of 14.97–14.52 ppm, which shifts upfield compared to the tri-coordinated chiral dioxaborinanes **($T_{(1-2)}B_{(1-2)}$)** because the boron atom completely adopts a tetrahedral configuration upon associating with 4-*tert*-butyl pyridine.

Further confirmation for the formation of ligands **(T_1** and **T_2)** and their chiral dioxaborinane complexes **($T_{(1-2)}B_{(1-2)}$)** and **($T_{(1-2)}B_{(1-2)}$-N)** comes from LC–MS/MS (Figure 3-5 and S23-S29 in the ESI). The LC–MS/MS spectra showed the expected molecular and fragmentation ions, with appropriate isotope distribution. The isotopic distribution of parent ions in the spectra demonstrated the presence of one boron atom in the chiral dioxaborinane complexes. The LC–MS/MS spectra of ligands **(T_1** and **T_2)** exhibit the ion peaks at m/z = 256.10 and 242.10 amu $[M + H]^+$ for **(T_1)** and **(T_2)**, respectively. On the other hand, the chiral dioxaborinanes complexes **($T_{(1-2)}B_{(1-2)}$)** and **($T_{(1-2)}B_{(1-2)}$-N)** show characteristic base peaks for the chiral dioxaborinane as $[M + H]^+$ or as $[M]^+$ and expected values.

3.3 | Catalytic performances of chiral dioxaborinane compounds

Nowadays, several transition metals such as Ir, Rh and Ru are often used as catalysts in transfer hydrogenation with high activity.[52–55] Instead of them; the development of the effective and cheaper catalytst for transfer hydrogenation of ketones is one of the main targets for the scientists, there have been continuous studies to

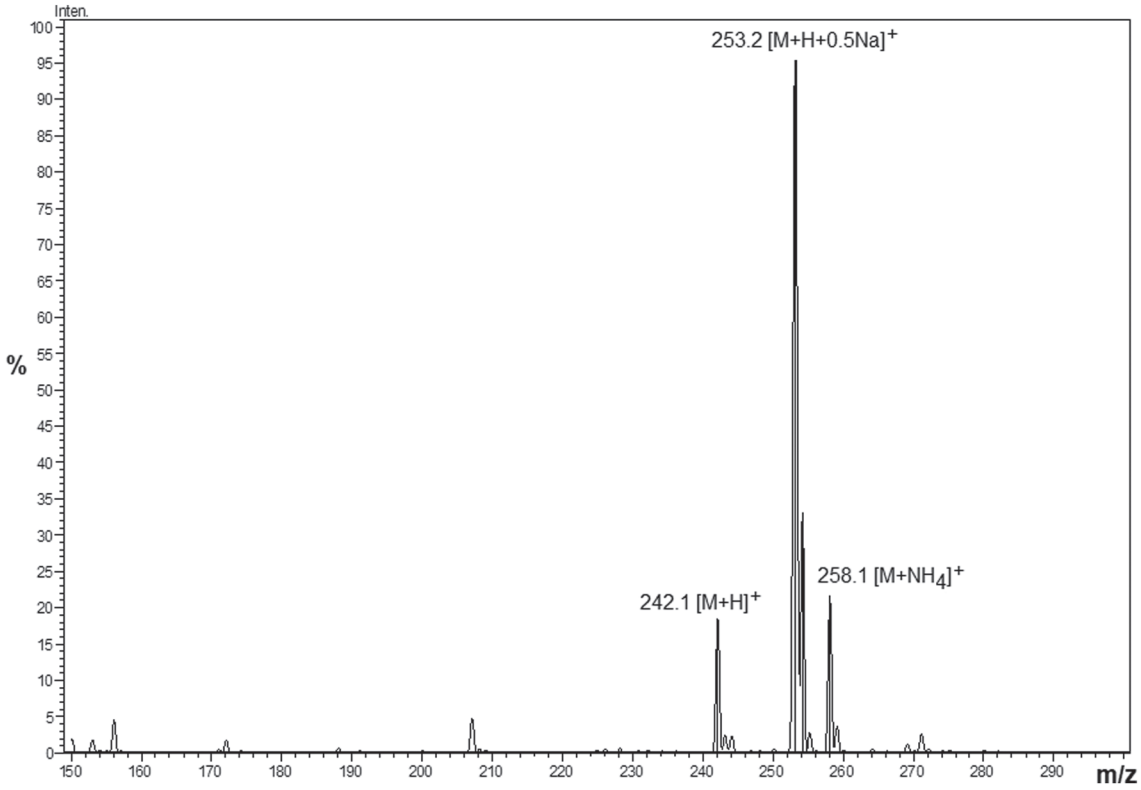

FIGURE 3 LC–MS/MS spectrum of chiral ligand **(T_2)**

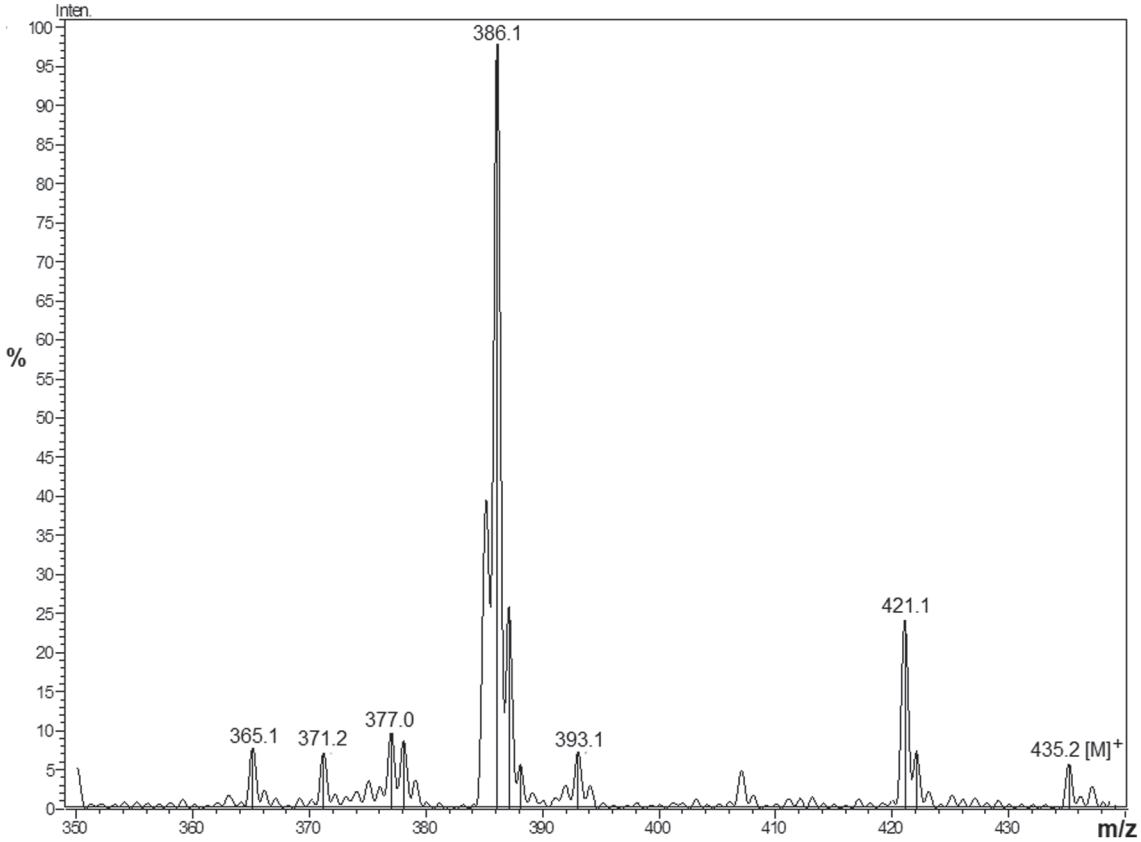

FIGURE 4 LC–MS/MS spectrum of dioxaborinane compound **(T_2B_1)**

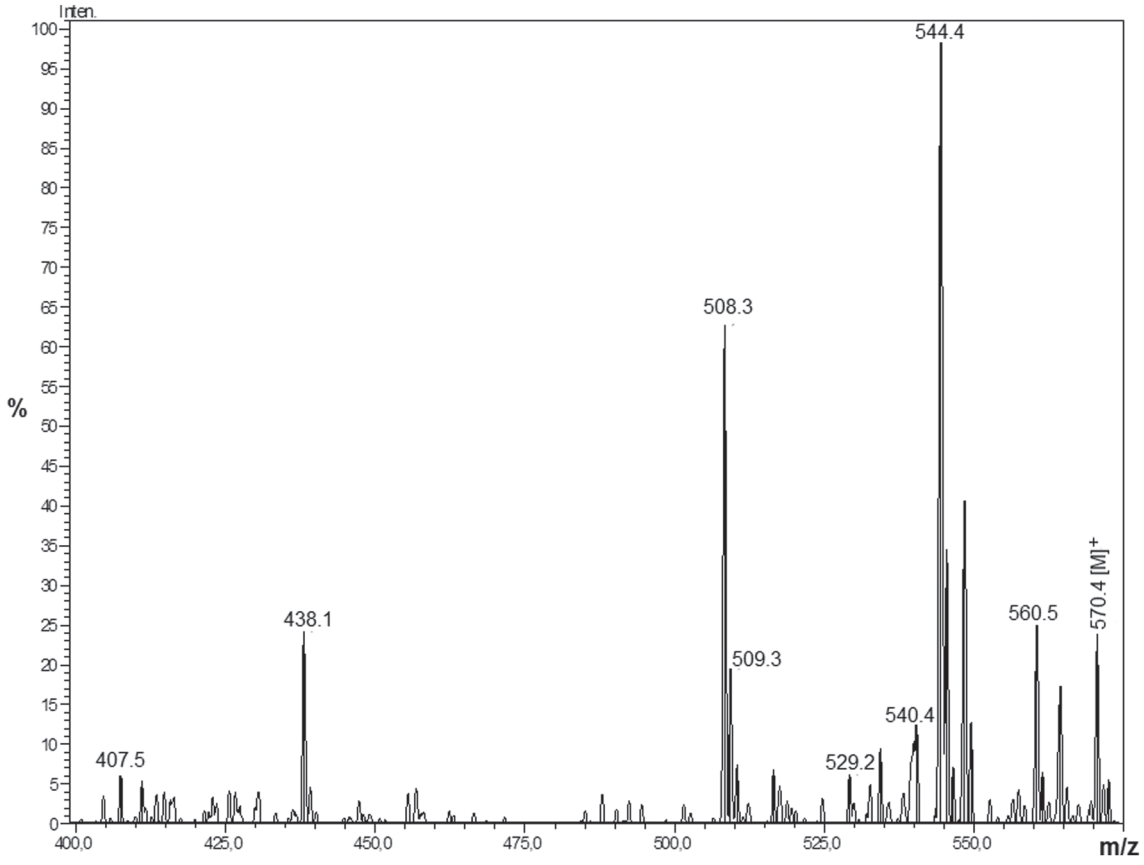

FIGURE 5 LC–MS/MS spectrum of chiral dioxaborinane compound **(T_2B_1-N)**

explore new metals for transfer hydrogenation reactions. In this study, we focused the use of boron metal for transfer hydrogenation. The asymmetric transfer hydrogenation (ATH) of ketones was studied with dioxaborinanes **($T_{(1-2)}B_{(1-2)}$)** and **($T_{(1-2)}B_{(1-2)}$-N)** as catalysts. In our initial experiment, acetophenone was used as a model substrate for the asymmetric transfer hydrogenation (ATH) and results of optimization studies were tabulated in Table 1. The optimization reactions were carried out under anaerobic conditions. Initially, we have taken acetophenone (0.5 mmol), *iso*-PrOH (5 ml) as the H-donor, NaOH (0.025 mmol) as the base and catalyst (0.005 mmol) at room temperature and stirred for 72 hr which results in lower conversions (Table 1, Entry 1–8). Due to the reversibility at room temperature, prolonging the reaction time led to a slight decrease in enantioselectivity (entries 1 and 2,[d]).[52–54] The next reaction was carried out without base and refluxed for 48 hr (Table 1, Entry 9–16) which results in no product formation. This indicates that the presence of a base is essential to carry out this reaction. In the ruthenium-catalyzed reaction, it was found that base abstracts proton of the alcohol, which makes the formation of ruthenium alkoxide easier and this alkoxide then undergoes β-elimination to afford ruthenium hydride, which is an active species in this reaction. This is the mechanism proposed by several research groups on the studies of ruthenium-catalyzed transfer hydrogenation reaction by metal hydride intermediates.[56–62] Boron-catalyzed mechanism is thought to be like this mechanism. The highest conversions were obtained when reactions were performed with a base at reflux temperature using catalysts **T_1B_2** and **T_1B_2-N** for 48 and 24 hr, respectively, as seen in Table 1, entry 17–24. Furthermore, we found that catalytic activity of complex **T_1B_1** and **T_2B_1**, which is only one methylene moiety different, is similar at the same temperature for the same reaction time (Entry 17–18). Moreover, substitution of 3,5-bis (trifluoromethyl)phenyl moiety **(T_1B_2** and **T_2B_2)** with ferrocene group does not cause any change in conversion, while slight change in enantioselectivity occurred (Entry 19–20). However, the coordination of 4-tert-butylpyridine to the boron atom led to an increase in both the reaction rate and enentioselectivity (Entry 21–24). In addition, there was no significant change in the conversion and enantioselectivity when KOH was used instead of NaOH (entry 17–18). Next, ratio of the base was changed from 100:1:3 to 100:1:9, and the highest conversion and

TABLE 1 Asymmetric Transfer hydrogenation of acetophenone with *iso*-PrOH catalyzed by tri-coordinated chiral dioxaborinanes **($T_{(1-2)}B_{(1-2)}$)** and four-coordinated chiral dioxaborinanes **($T_{(1-2)}B_{(1-2)}$-N)**

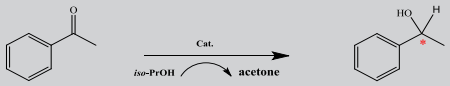

Entry	Complex	S/C/NaOH	Time	Conversion(%)[f]	%ee[g]	Configuration[h]
1	T_1B_1[a]	100:1:5	72 hr (144 h)[d]	12 (24)[d]	12 (8)[d]	*S*
2	T_2B_1[a]	100:1:5	72 hr (144 h)[d]	13 (24)[d]	13 (8)[d]	*S*
3	T_1B_2[a]	100:1:5	72	13	10	*S*
4	T_2B_2[a]	100:1:5	72	14	10	*S*
5	T_1B_1N[a]	100:1:5	72	26	35	*S*
6	T_2B_1N[a]	100:1:5	72	25	34	*S*
7	T_1B_2N[a]	100:1:5	72	22	22	*S*
8	T_2B_2N[a]	100:1:5	72	28	23	*S*
9	T_1B_1[b]	100:1	48 hr (48 hr)[e]	< 3	--	--
10	T_2B_1[b]	100:1	48 hr (48 hr)[e]	< 3	--	--
11	T_1B_2[b]	100:1	48 hr	< 3	--	--
12	T_2B_2[b]	100:1	48 hr	< 3	--	--
13	T_1B_1N[b]	100:1	48 hr	< 3	--	--
14	T_2B_1N[b]	100:1	48 hr	< 3	--	--
15	T_1B_2N[b]	100:1	48 hr	< 3	--	--
16	T_2B_2N[b]	100:1	48 hr	< 3	--	--
17	T_1B_1[c]	100:1:5	48 hr	97 (98)[e]	16 (14)[e]	*S*
18	T_2B_1[c]	100:1:5	48 hr	98 (98)[e]	16 (14)[e]	*S*
19	T_1B_2[c]	100:1:5	48 hr	99	11	*S*
20	T_2B_2[c]	100:1:5	48 hr	97	11	*S*
21	T_1B_1N[c]	100:1:5	24 hr	98	38	*S*
22	T_2B_1N[c]	100:1:5	24 hr	98	40	*S*
23	T_1B_2N[c]	100:1:5	24 hr	97	28	*S*
24	T_2B_2N[c]	100:1:5	24 hr	99	30	*S*
25	T_1B_1N[d]	100:1:3	24 hr	92	33	*S*
26	T_1B_1N[d]	100:1:5	24 hr	98	38	*S*
27	T_1B_1N[d]	100:1:7	24 hr	94	35	*S*
28	T_1B_1N[d]	100:1:9	24 hr	94	33	*S*

Reaction conditions
[a]At room temperature; acetophenone/Cat./NaOH, 100:1:5;
[b]Refluxing in *iso*PrOH; acetophenone/Cat., 100:1, in the absence of base;
[c]Refluxing in *iso*PrOH; acetophenone/Cat./NaOH, 100:1:5;
[d]At room temperature; acetophenone/Cat./NaOH, 100:1:5, (64 hr);
[e]Refluxing in *iso*PrOH; acetophenone/Cat./KOH, 100:1:5;
[f]Determined by GC (three independent catalytic experiments);
[g]Determined by capillary GC analysis using a chiral cyclodex B (Agilent) capillary column;
[h]Determined by comparison of the retention times of the enantiomers on the GC traces with literature values.

enantioselectivity were obtained with a base ratio of 100:1:5 (Entry 25–28). Having established the optimum reaction conditions, we set out to explore the substrate generality of the asymmetric transfer hydrogenation of acetophenone derivatives. The introduction of electron-withdrawing substituents, such as F, Cl, Br or NO_2, on

TABLE 2 Asymmetric Transfer Hydrogenation results for substituted acetophenones catalyzed by tri-coordinated chiral dioxaborinanes **($T_{(1-2)}B_{(1-2)}$)** and four-coordinated chiral dioxaborinanes **($T_{(1-2)}B_{(1-2)}$-N)**[a]

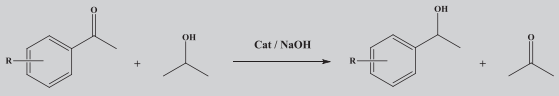

Entry	Catalyst	Substrate	Product	Time	Conv.(%)[b]	ee(%)[c]	Config.[d]
1	T_1B_1			16 hr	98	15	*S*
2	T_2B_1			16 hr	98	15	*S*
3	T_1B_2	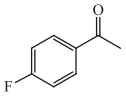	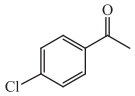	16 hr	98	12	*S*
4	T_2B_2			16 hr	96	13	*S*
5	T_1B_1N			8 hr	97	37	*S*
6	T_2B_1N			8 hr	99	38	*S*
7	T_1B_2N			8 hr	98	28	*S*
8	T_2B_2N			8 hr	99	28	*S*
9	T_1B_1			24 hr	98	14	*S*
10	T_2B_1			24 hr	97	13	*S*
11	T_1B_2	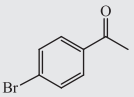	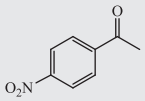	24 hr	97	12	*S*
12	T_2B_2			24 hr	99	11	*S*
13	T_1B_1N			12 hr	98	36	*S*
14	T_2B_1N			12 hr	99	36	*S*
15	T_1B_2N			12 hr	99	25	*S*
16	T_2B_2N			12 hr	98	26	*S*
17	T_1B_1			30 hr	96	13	*S*
18	T_2B_1			30 hr	97	12	*S*
19	T_1B_2	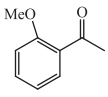	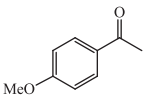	30 hr	98	10	*S*
20	T_2B_2			30 hr	99	11	*S*
21	T_1B_1N			16 hr	98	36	*S*
22	T_2B_1N			16 hr	99	36	*S*
23	T_1B_2N			16 hr	97	24	*S*
24	T_2B_2N			16 hr	98	26	*S*
25	T_1B_1			16 hr	98	11	*S*
26	T_2B_1			16 hr	99	11	*S*
27	T_1B_2	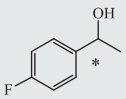	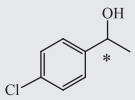	16 hr	99	10	*S*
28	T_2B_2			16 hr	99	10	*S*
29	T_1B_1N			8 hr	97	33	*S*
30	T_2B_1N			8 hr	96	33	*S*
31	T_1B_2N			8 hr	98	23	*S*
32	T_2B_2N			8 hr	98	25	*S*
33	T_1B_1			3 days	98	16	*S*
34	T_2B_1			3 days	99	17	*S*
35	T_1B_2	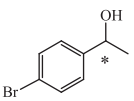	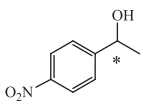	3 days	99	13	*S*
36	T_2B_2			3 days	99	12	*S*
37	T_1B_1N			3/2 days	97	41	*S*

(Continues)

TABLE 2 (Continued)

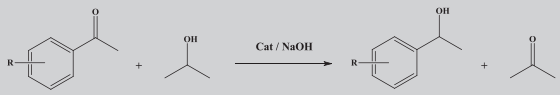

Entry	Catalyst	Substrate	Product	Time	Conv.(%)[b]	ee(%)[c]	Config.[d]
38	$\mathbf{T_2B_1N}$			3/2 days	97	43	*S*
39	$\mathbf{T_1B_2N}$			3/2 days	96	30	*S*
40	$\mathbf{T_2B_2N}$			3/2 days	98	32	*S*
41	$\mathbf{T_1B_1}$			6 days	97	10	*S*
42	$\mathbf{T_2B_1}$	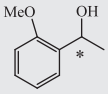	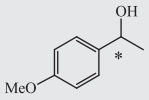	6 days	99	10	*S*
43	$\mathbf{T_1B_2}$			6 days	97	10	*S*
44	$\mathbf{T_2B_2}$			6 days	96	10	*S*
45	$\mathbf{T_1B_1N}$			3 days	96	32	*S*
46	$\mathbf{T_2B_1N}$			3 days	99	32	*S*
47	$\mathbf{T_1B_2N}$			3 days	97	20	*S*
48	$\mathbf{T_2B_2N}$			3 days	99	23	*S*

Reaction conditions

[a]Catalyst (0.005 mmol), substrate (0.5 mmol), *iso*-PrOH (5 ml), NaOH (0.025 mmol %), 82 °C, the concentration of acetophenone derivatives is 0.1 M;

[b]Purity of compounds is checked by ^{1}H NMR and GC (three independent catalytic experiments), yields are based on aryl ketone;

[c]Determined by capillary GC analysis using a chiral cyclodex B (Agilent) capillary column (30 m x 0.32 mm I.D. x 0.25 μm film thickness);

[d]Determined by comparison of the retention times of the enantiomers on the GC traces with literature values.

the 4-position of the phenyl ring of the acetophenone derivatives resulted in improved activity, while there was no significant change in enantioselectivity (Entries 1–32, Table 2). The introduction of electron-withdrawing substituents to the *para* position of the phenyl ring of the ketone decreased the electron density of the C=O bond so that the activity was improved giving rise to easier hydrogenation and undergoes hydrogenation faster than that of acetophenone.[55,63,64] Furthermore, the influence of positions of electron-donating groups on transfer hydrogenation was studied. It appears that the conversions and enantioselectivities are sensitive for the position of electron-donating substituents on the phenyl ring. Both conversion and enantioselectivity are higher for *ortho*-methoxy substituted acetophenone than those for *para*-methoxy substituted one (Entry 33–48).

As seen in Table 3, complex $\mathbf{T_1B_1}$**-N** catalyzed the reduction of aryl/alkyl and alkyl/alkyl ketones to their corresponding alcohols with >95% conversion. These ketones took a longer time to react compared to acetophenone derivatives. Furthermore, a variety of simple alkyl/alkyl ketones were transformed into the corresponding secondary alcohols and it was found that the activity and selectivity were highly dependent on the steric hindrance of the alkyl group. Namely, when the size of the alkyl group increased, the activity and selectivity decreased (Entry 1–4). In addition, as can be seen from Entry 5, 1-naphthyl methyl ketone was reduced with the highest conversion and enantioselectivity. When entries 7 and 8 were considered, the replacement of CH_3 with C_6H_5 in the ketone decreases reaction rate.

3.4 | Biological activities

3.4.1 | DPPH radical scavenging activity

The decrease in the absorbance of the DPPH radical occurs during the incubation period. This is because antioxidants take hydrogen from radicals or give electrons. Due to this feature, DPPH is often used as a substrate to evaluate the antioxidant activity of organic and inorganic substances.[65] As shown in Figure 6, all chiral dioxaborinane complexes showed different rates of radical scavenging activity. The dioxaborinane $\mathbf{T_2B_2N}$ exhibited the highest activity among all chiral dioxaborinane complexes. When the concentration of this dioxaborinane complex was increased from 25.0 μg/ml to

TABLE 3 Asymmetric Transfer Hydrogenation results for various ketones catalyzed chiral dioxaborinane $\mathbf{T_2B_1N}$[a]

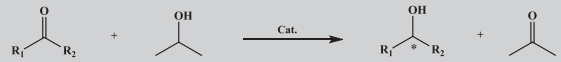

Entry	Complex	R_1	R_2	Time (Days)	Conv.(%)[b]	ee(%)[c]	Config.[d]
1	$\mathbf{T_2B_1N}$	CH_3	CH_2CH_3	2	96	36	*S*
2	$\mathbf{T_2B_1N}$	CH_3	$CH_2CH_2C_6H_5$	3	98	32	*S*
3	$\mathbf{T_2B_1N}$	CH_3	$CH\ (CH_3)_2$	8	97	32	*S*
4	$\mathbf{T_2B_1N}$	CH_3	$CH_2CH(CH_3)_2$	6	98	30	*S*
5	$\mathbf{T_2B_1N}$	CH_3	1-naphthyl	3/2	98	42	*S*
6	$\mathbf{T_2B_1N}$	CH_3	$n\text{-}C_4H_9$	5	97	27	*S*
7	$\mathbf{T_2B_1N}$	CH_3	C_6H_{11}	3	96	22	*S*
8	$\mathbf{T_2B_1N}$	C_6H_5	C_6H_{11}	6	98	25	*S*

Reaction conditions:
[a]Catalyst (0.005 mmol), substrate (0.5 mmol), *iso*PrOH (5 ml), NaOH (0.025 mmol %), 82 °C, the concentration of ketones is 0.1 M;
[b]Purity of compounds is checked by ^{1}H NMR and GC (three independent catalytic experiments), yields are based on aryl ketone;
[c]Determined by capillary GC analysis using a chiral cyclodex B (Agilent) capillary column (30 m x 0.32 mm I.D. x 0.25 μm film thickness);
[d]Determined by comparison of the retention times of the enantiomers on the GC traces with literature values.

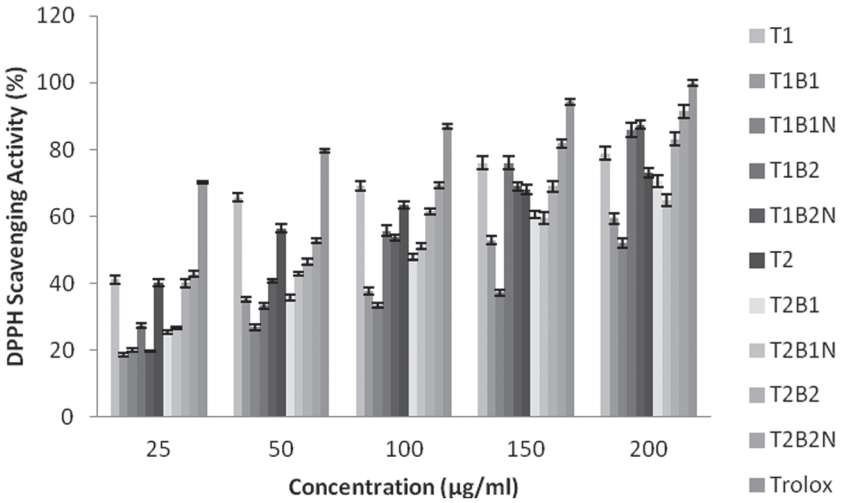

FIGURE 6 Free radical scavenging activities of chiral dioxaborinane compounds

200.0 μg/ml, the scavenging rate increased from 42.8 ± 0.83% to 91.4 ± 1.97%. The order of scavenging capacity of the chiral dioxaborinane compounds at 200 μg/ml concentration was determined as $\mathbf{T_2B_2N > T_1B_2N > T_1B_2 > T_2B_2 > T_1 > T_2 > T_2B_1 > T_2B_1N > T_1B_1 > T_1B_1N}$. At high concentrations, $\mathbf{T_2B_2N}$ exhibited activity close to Trolox, which is used as a standard reference substance.

3.4.2 | Reducing power activity

Compounds with reducing power can be used as antioxidants to reduce oxidative intermediates in lipid peroxidation.[66] As shown in Figure 7, all chiral dioxaborinane complexes exhibited different rates of reducing power activity. It was observed that as the concentration of the test compounds increased, the activity of reducing power also increased. Among the chiral dioxaborinane complexes, the highest reducing power activity was observed in $\mathbf{T_1B_2}$ (0.647 ± 0.011) and $\mathbf{T_2B_2}$ (0.629 ± 0.013) at the concentration of 200.0 μg/ml, while the lowest activity in the same concentration was detected in $\mathbf{T_1B_1N}$ (0.357 ± 0.015) and $\mathbf{T_2B_1N}$ (0.292 ± 0.009). The α-tocopherol used as a standard showed higher activity than the complexes at all concentrations studied.

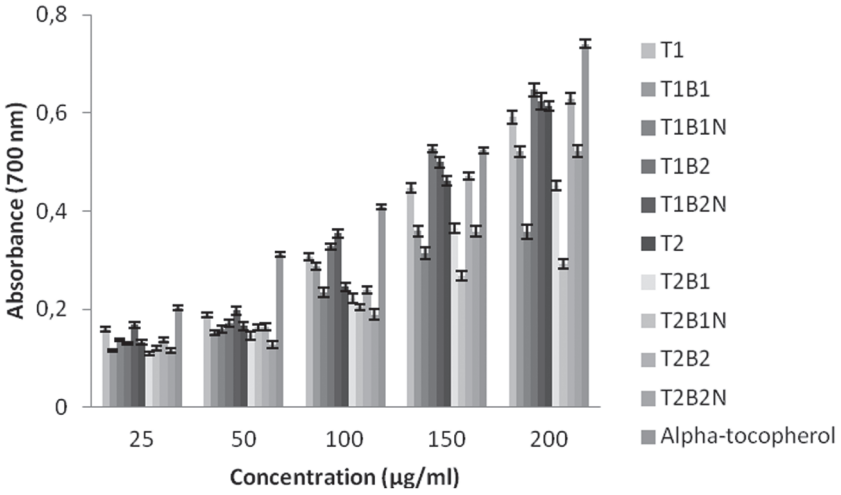

FIGURE 7 Reducing power activities of chiral dioxaborinane compounds

3.4.3 | Antibacterial activity

The antibacterial activity of new chiral dioxaborinane compounds was tested against three Gram+ and three Gram-bacteria. Among the chiral dioxaborinane compounds, only $\mathbf{T_1B_2}$ (500 µg/ml) exhibited weak antibacterial activity against two bacteria, while the other chiral dioxaborinane compounds did not have any activity. The chiral dioxaborinane $\mathbf{T_1B_2}$ formed an inhibition zone of 9 mm against *L. pneumophila* and 7 mm against *E. hirae*. Streptomycin and Tetracycline showed 15 mm and 21 mm inhibition zone against *L. pneumophila*, while they showed 19 mm and mm 22, respectively, against *E. hirae*.

3.4.4 | DNA binding activity

The movement of molecules in the agarose gel electrophoresis method depends on their mass, charge, and shape.[67] Due to the binding of CT-DNA to the compounds, free DNA moves faster on the gel since it is smaller than the bound DNA.[68] Agarose gel electrophoresis results of CT-DNA bound complexes are given in Figure 8. According to the results, it was determined that $\mathbf{T_1}$, $\mathbf{T_1B_1}$ and $\mathbf{T_2}$ having little movement on the gel, had high DNA binding capacity, while $\mathbf{T_1B_2N}$, $\mathbf{T_2B_1}$, and $\mathbf{T_2B_2N}$ had low DNA binding capacity.

3.4.5 | DNA cleavage activity

When super-helical plasmid pBR322 is run under normal conditions on DNA gel electrophoresis, a single band is observed on the gel. However, if super-helix DNA (form I) is subjected to an external effect, its one or two chains may break. In a break in a single chain, two bands appear (Form I and Form II) on the gel. When a break in two chains occurs, three bands (Form I, Form II and Form III) appear on the gel. The slowest moving

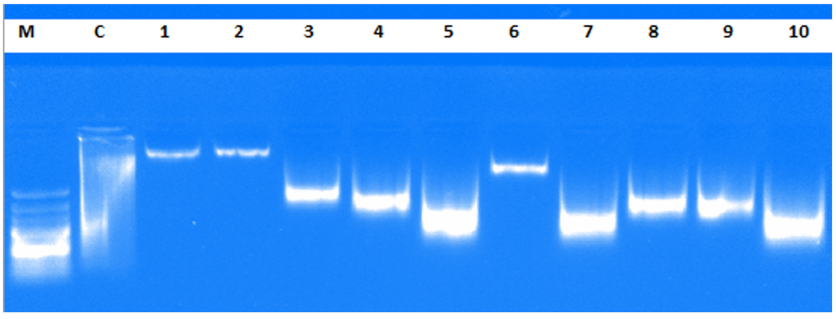

FIGURE 8 DNA binding activity of chiral dioxaborinane compounds. Lane M, DNA Marker; Lane C, Kontrol, CT- DNA; Lane 1, CT-DNA + 200 µg/ml T_1; Lane 2, CT- DNA + 200 µg/ml T_1B_1; Lane 3, CT- DNA + 200 µg/ml T_1B_1N; Lane 4, CT- DNA + 200 µg/ml T_1B_2; Lane 5, CT- DNA + 200 µg/ml T_1B_2N; Lane 6, CT- DNA + 200 µg/ml T_2; Lane 7, CT- DNA + 200 µg/ml T_2B_1; Lane 8, CT- DNA + 200 µg/ml T_2B_1N; Lane 9, CT- DNA + 200 µg/ml T_2B_2; Lane 10, CT- DNA + 200 µg/ml T_2B_2N

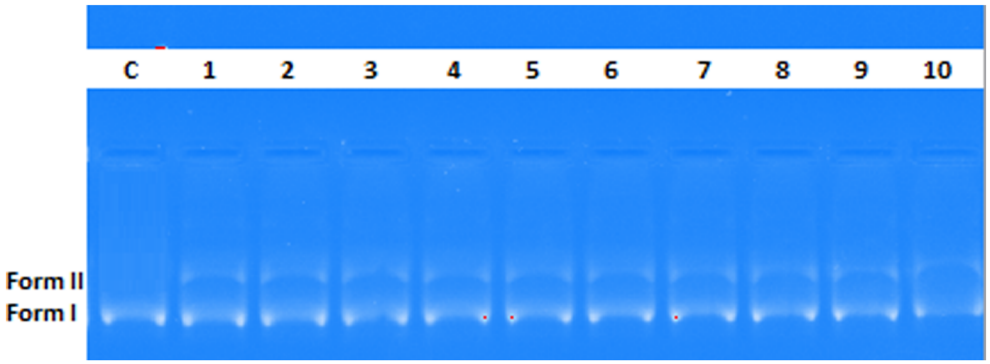

FIGURE 9 DNA Cleavage activity of chiral dioxaborinane compounds. Lane C, Control, pBR 322 DNA; Lane 1, pBR 322 DNA + 200 μg/ml T_1; Lane 2, pBR 322 DNA + 200 μg/ml T_1B_1; Lane 3, pBR 322 DNA + 200 μg/ml T_1B_1N; Lane 4, pBR 322 DNA + 200 μg/ml T_1B_2; Lane 5, pBR 322 DNA + 200 μg/ml T_1B_2N; Lane 6, pBR 322 DNA + 200 μg/ml T_2; Lane 7, pBR 322 DNA + 200 μg/ml T_2B_1; Lane 8, pBR 322 DNA + 200 μg/ml T_2B_1N; Lane 9, pBR 322 DNA + 200 μg/ml T_2B_2; Lane 10, pBR 322 DNA + 200 μg/ml T_2B_2N

structure is Form II, while the fastest moving structure is Form I. Form III is positioned between these two structures.[69] The electrophoresis results of the 200 mg/ml concentration of chiral dioxaborinane compounds after incubation with supercoiled plasmid pBR322 DNA are given in Figure 9. According to the results, a band (Form I) was obtained for the control untreated with compounds (Lane C) and two bands (Form I and II) from the samples treated with the compounds (Lane 1–10). All the newly synthesized dioxaborinane compounds were determined to exhibit one strand cleavage activity of supercoiled DNA.

4 | CONCLUSION

In this study, we synthesized two new *cis*-1,2-diol-type chiral ligands **(T_1** and **T_2)** and their tri-coordinated chiral dioxaborinane **($T_{(1-2)}B_{(1-2)}$)** and four-coordinated chiral dioxaborinane adducts with 4-*tert*-butyl pyridine sustained by N → B dative bonds **($T_{(1-2)}B_{(1-2)}$-N)**. Two chiral ligands and their chiral dioxaborinane complexes were characterized by the FT-IR, UV–Vis, and NMR (^{1}H, ^{13}C, and ^{11}B) spectroscopy, LC–MS/MS, and elemental analysis. The chiral dioxaborinane complexes were also used as catalyst for the asymmetric transfer hydrogenation (ATH) of acetophenone derivatives under suitable conditions. The catalytic results show that the chiral dioxaborinane complexes are good catalyst precursors. In tests to determine the biological activities of newly synthesized chiral dioxaborinane complexes, it was determined that almost all the chiral dioxaborinane complexes have antioxidant activity. The **T_2B_2N** exhibited the highest radical scavenging activity among the complexes. Except for the weak antibacterial effect exhibited by **T_1B_2**, the complexes had no antibacterial effect. It has also been shown that complexes have different rates of DNA binding activity and can break super-helix DNA from a single chain.

ACKNOWLEDGEMENT

We acknowledge gratefully the financial support from Research Fund of Harran University (*HUBAP Projects No: 19023)* Sanliurfa, Turkey.

CONFLICT OF INTEREST

The authors declare that they have no conflict of interest.

ORCID

Ahmet Kilic https://orcid.org/0000-0001-9073-4339
Murat Aydemir https://orcid.org/0000-0002-4238-5012
Feyyaz Durap https://orcid.org/0000-0003-0899-1948

REFERENCES

[1] J. Cruz-Huerta, G. Campillo-Alvarado, H. Höpfl, P. Rodriguez-Cuamatzi, V. R. Marquez, J. Guerrero-Álvarez, D. Salazar-Mendoza, N. Farfán-García, *Eur. J. Inorg. Chem.* **2016**, 355.
[2] L. Zhu, S. H. Shabbir, M. Gray, V. M. Lynch, S. Sorey, E. V. Anslyn, *J. Am. Chem. Soc.* **2006**, *128*, 1222.
[3] S. Kusano, S. Konishi, Y. Yamada, O. Hayashida, *Org. Biomol. Chem.* **2018**, *16*, 4619.
[4] N. Christinat, R. Scopelliti, K. Severin, *J. Org. Chem.* **2007**, *72*, 2192. and references therein
[5] N. Christinat, R. Scopelliti, K. Severin, *Angew. Chem., Int. Ed.* **2008**, *47*, 1848. and references therein
[6] E. Sheepwash, K. Zhou, R. Scopelliti, K. Severin, *Eur. J. Inorg. Chem.* **2013**, *2013*, 2558.
[7] J. Kua, M. N. Fletcher, P. M. Iovine, *J. Phys. Chem.* **2006**, *110*, 8158.
[8] J. Beckmann, D. Dakternieks, A. Duthie, A. E. K. Lim, E. R. T. Tiekink, *J. Organomet. Chem.* **2001**, *633*, 149.
[9] J. L. Kolanowski, F. Liu, E. J. New, *Chem. Soc. Rev.* **2018**, *47*, 195.

[10] T. G. Drummond, M. G. Hill, J. K. Barton, *Nat. Biotechnol.* **2003**, *21*, 1192.

[11] E. Katz, A. Bückmann, I. Willner, *J. Am. Chem. Soc.* **2001**, *123*, 10752.

[12] F. L. Rock, W. Mao, A. Yaremchuk, M. Tukalo, T. Crépin, H. Zhou, Y.-K. Zhang, V. Hernandez, T. Akama, S. J. Baker, J. J. Plattner, L. Shapiro, S. A. Martinis, S. J. Benkovic, S. Cusack, M. R. K. Alley, *Science* **2007**, *316*, 1759.

[13] E. Sonoiki, C. L. Ng, M. C. S. Lee, D. Guo, Y.-K. Zhang, Y. Zhou, M. R. K. Alley, V. Ahyong, L. M. Sanz, M. J. Lafuente-Monasterio, C. Dong, P. G. Schupp, J. Gut, J. Legac, R. A. Cooper, F.-J. Gamo, J. DeRisi, Y. R. Freund, D. A. Fidock, P. J. Rosenthal, *Nat. Commun.* **2017**, *8*, 14574.

[14] P. Eisenberger, C. M. Crudden, *Dalton Trans.* **2017**, *46*, 4874.

[15] A. Kilic, I. H. Kaya, I. Ozaslan, M. Aydemir, F. Durap, *Catal. Commun.* **2018**, *111*, 42. and references therein

[16] A. Kilic, E. Yasar, E. Aytar, *Sustainable Energy Fuels* **2019**, *3*, 1066. and references therein.

[17] J. Lam, B. A. R. Günther, J. M. Farrell, P. Eisenberger, B. P. Bestvater, P. D. Newman, R. L. Melen, C. M. Crudden, D. W. Stephan, *Dalton Trans.* **2016**, *45*, 15303.

[18] F. Yang, M. Zhu, J. Zhang, H. Zhou, *Med. Chem. Commun.* **2018**, *9*, 201.

[19] S. Pasa, O. Erdogan, C. Yenisey, *J. Mol. Struct.* **2019**, *1186*, 458.

[20] T. M. Percino, J. E. G. Ramírez, E. M. Jimenez, C. R. T. Munoz, *J. Organomet. Chem.* **2019**, *891*, 35.

[21] H. S. Ban, H. Nakamura, *Chem. Rec.* **2015**, *15*, 616.

[22] R. Smoum, A. Rubinstein, V. M. Dembitsky, M. Srebnik, *Chem. Rev.* **2012**, *112*, 4156.

[23] L. Ciani, S. Ristori, *Expert Opin. Drug Discovery* **2012**, *7*, 1017.

[24] V. Jangir, J. Sharma, R. Avatar Sharma, Y. Singh, *Main Group Met. Chem.* **2016**, *39*, 9.

[25] A. Kilic, M. Durgun, F. Durap, M. Aydemir, *J. Organomet. Chem.* **2019**, *890*, 1.

[26] A. Kilic, O. Ozbahceci, M. Durgun, M. Aydemir, *Polycyclic Aromat. Compd.* **2019**, *39*, 248.

[27] Y. Tülüce, H. D. I. Masseh, I. Koyuncu, A. Kilic, M. Durgun, H. Özkol, *Anti-Cancer Agents Med. Chem.* **2019**, *19*, 627.

[28] A. Kilic, I. Koyuncu, M. Durgun, I. Ozaslan, I. H. Kaya, A. Gonel, *Chem. Biodiversity* **2018**, *15*, e1700428.

[29] Y. Kitamoto, F. Kobayashi, T. Suzuki, Y. Miyata, H. Kita, K. Funakic, S. Oi, *Dalton Trans.* **2019**, *48*, 2118.

[30] G. Campillo-Alvarado, E. C. Vargas-Olvera, H. Höpfl, A. D. Herrera-Espana, O. Sanchez-Guadarrama, H. Morales-Rojas, L. R. MacGillivray, B. Rodríguez-Molina, N. Farfan, *Cryst. Growth des.* **2018**, *18*, 2726.

[31] J. Tan, A. B. Cognetta III, D. B. Diaz, K. M. Lum, S. Adachi, S. Kundu, B. F. Cravatt, A. K. Yudin, *Nat. Commun.* **2017**, *8*, 1760.

[32] E. Meiyanto, R. A. Susidarti, R. I. Jenie, R. Y. Utomo, D. Novitasari, F. Wulandari, M. Kirihata, *J. Appl. Pharm. Sci.* **2020**, *10*, 60.

[33] S. Gronowitz, T. Dahlgren, J. Namtvedt, C. Roos, B. Sjoberg, U. Forsgren, *Acta Pharm. Suec.* **1971**, *8*, 377.

[34] P. C. Trippier, C. McGuigan, *MedChemComm.* **2010**, *1*, 183.

[35] S. Touchet, F. Carreaux, B. Carboni, A. Bouillon, J.-L. Boucher, *Chem. Soc. Rev.* **2011**, *40*, 3895.

[36] X. Chen, S. Schauder, V. Potier, A. Van Dorsselaer, I. Pelczer, B. L. Bassler, F. M. Hughson, *Nature* **2002**, *415*, 545.

[37] E. S. Priestley, I. De Lucca, B. Ghavimi, S. Erickson-Viitanen, C. P. Decicco, *Bioorg. Med. Chem. Lett.* **2002**, *12*, 3199.

[38] D. S. Raja, N. S. Bhuvanesh, K. Natarajan, *Dalton Trans.* **2012**, *41*, 4365.

[39] H. Baykara, S. Ilhan, A. Levent, M. S. Seyitoglu, S. Ozdemir, V. Okumus, A. Oztomsuk, M. Cornejo, *Spectrochim. Acta a* **2014**, *13*, 270.

[40] M. Oyaizu, *Japanese Journal of Nurition* **1986**, *44*, 307.

[41] S. A. Khan, A. M. Asiri, *J. Heterocycl. Chem.* **2012**, *49*, 1452.

[42] N. Meriç, C. Kayan, K. Rafikova, A. Zazybin, V. Okumus, M. Aydemir, F. Durap, *Chem. Pap.* **2019**, *73*, 1199.

[43] E. Tas, A. Kilic, N. Konak, I. Yilmaz, *Polyhedron* **2008**, *27*, 1024.

[44] K. A. Ketuly, A. H. A. Hadi, *Molecules* **2010**, *15*, 2347.

[45] S. J. Cassidy, I. Brettell-Adams, L. E. McNamara, M. F. Smith, M. Bautista, H. Cao, M. Vasiliu, D. L. Gerlach, F. Qu, N. I. Hammer, D. A. Dixon, P. A. Rupar, *Organometallics* **2018**, *37*, 3732.

[46] X. Cao, C. Wu, Y. Tian, P. Guo, *RSC Adv.* **2019**, *9*, 12247.

[47] X. Zeng, S. Poppe, A. Lehmann, M. Prehm, C. Chen, F. Liu, H. Lu, G. Ungar, C. Tschierske, *Angew. Chem. Int. Ed.* **2019**, *58*, 1.

[48] M. Shaker, S. Adam, O. M. El-Hady, F. Ullah, *RSC Adv.* **2019**, *9*, 34311.

[49] P. M. Garcia-Barrantes, G. V. Lamoureux, A. L. Perez, R. N. Garcia-Sanchez, A. R. Martinez, A. S. Feliciano, *Eur. J. Med. Chem.* **2013**, *70*, 548.

[50] M. Ibarra-Rodriguez, B. M. Muñoz-Flores, H. V. R. Dias, M. Sanchez, A. Gomez-Trevinno, R. Santillan, N. Farfan, V. M. Jimenez-Perez, *J. Org. Chem.* **2017**, *82*, 2375.

[51] J. Guillon, S. Moreau, E. Mouray, V. Sinou, I. Forfar, S. B. Fabre, V. Desplat, P. Millet, D. Parzy, C. Jarry, P. Grellier, *Bioorg. Med. Chem.* **2008**, *16*, 9133.

[52] F. Durap, D. Elma Karakas, B. Ak, A. Baysal, M. Aydemir, *J. Organomet. Chem.* **2016**, *818*, 92.

[53] Y. W. A. Al-Bayati, D. Elma Karakas, N. Meric, M. Aydemir, F. Durap, A. Baysal, *Appl. Organomet. Chem.* **2018**, *32*, 3919.

[54] N. Meric, C. Kayan, M. Gürbüz, M. Karakaplan, N. Erkin Binbay, M. Aydemir, *Tetrahedron: Asymmetry* **2017**, *28*, 1739.

[55] F. Ok, M. Aydemir, F. Durap, A. Baysal, *Appl. Organomet. Chem.* **2014**, *28*, 38.

[56] J. E. Backvall, *J. Organomet. Chem.* **2002**, *652*, 105.

[57] R. Noyori, S. Hashiguchi, *Acc. Chem. Res.* **1997**, *30*, 97.

[58] H. Doucet, T. Ohkuma, K. Murata, T. Yokozawa, M. Kozawa, E. Katayama, F. A. England, T. Ikariya, R. Noyori, *Angew. Chem. Int. Ed.* **1998**, *37*(12), 1703.

[59] E. P. Kelson, P. P. Phengsy, *J. Chem. Soc. Dalton Trans.* **2000**, 4023.

[60] H. Zhang, C. B. Yang, Y. Y. Li, Z. R. Donga, Z. X. Gao, H. Nakamura, K. Murata, K. Ikariya, *Chem. Commun.* **2003**, 142.

[61] R. Nandhini, G. Venkatachalam, *J. Organomet. Chem.* **2019**, *895*, 15.

[62] N. Meric, F. Durap, M. Aydemir, A. Baysal, *Appl. Organomet. Chem.* **2014**, *28*, 803.

[63] J. W. Faller, A. R. Lavoie, *Organometallics* **2001**, *20*, 5245.

[64] N. Meric, M. Aydemir, *J. Organomet. Chem.* **2016**, *819*, 120.

[65] A. Gumus, V. Okumus, *Turk. J. Chem.* **2018**, *42*, 1344.

[66] T. T. Zhang, Y. J. Liu, L. Yang, J. G. Jiang, J. W. Zhao, W. Zhu, *Med. Chem. Commun.* **2017**, *8*, 1673.
[67] H. Keypour, A. Shooshtari, M. Rezaeivala, F. O. Kup, H. A. Rudbari, *Polyhedron* **2015**, *97*, 75.
[68] A. Gumus, V. Okumus, S. Gumus, *Turk. J. Chem.* **2018**, *42*, 1358.
[69] G. Devagi, F. Dallemer, P. Kalaivani, R. Prabhakaran, *J. Organomet. Chem.* **2018**, *854*, 1.

SUPPORTING INFORMATION

Additional supporting information may be found online in the Supporting Information section at the end of this article.

How to cite this article: Kilic A, Balci TE, Arslan N, et al. Synthesis of *cis*-1,2-diol-type chiral ligands and their dioxaborinane derivatives: Application for the asymmetric transfer hydrogenation of various ketones and biological evaluation. *Appl Organomet Chem*. 2020;e5835. https://doi.org/10.1002/aoc.5835